Characterizing PM$_{2.5}$ Emissions and Temporal Evolution of Organic Composition from Incense Burning in a California Residence

Jennifer Ofodile[1,], Michael R. Alves[1], Yutong Liang[1,†], Emily B. Franklin[2,‡], David M. Lunderberg[1,§], Cesunica E. Ivey[2], Brett C. Singer[3], William W Nazaroff[2], and Allen H. Goldstein[1,2]*

Corresponding Author: jofodile@berkeley.edu

[1]*Department of Environmental Science, Policy, and Management, University of California, Berkeley, Berkeley, CA 94720, United States*

[2]*Department of Civil and Environmental Engineering, University of California, Berkeley, Berkeley, CA 94720, United States*

[3]*Indoor Environment Group, Energy Analysis and Environmental Impacts Division, Building Technologies and Urban Systems Division, Energy Technologies Area, Lawrence Berkeley National Laboratory, Berkeley, CA 94720, United States*

[†]*Y.L.: Now at School of Chemical and Biomolecular Engineering, Georgia Institute of Technology, Atlanta, GA 30332, United States*

[‡]*E.B.F.: Now at Environment Unit, CSIRO, Aspendale 3195, Australia*

[§]*D.M.L.: Now at Office of Energy Efficiency & Renewable Energy, AAAS Science, Technology and Policy Fellow, U.S. Department of Energy, Washington, DC 20585, United States*

ABSTRACT

The chemical composition of incense-generated organic aerosol in residential indoor air has received limited attention in Western literature. In this study, we conducted incense burning experiments in a single-family California residence during vacancy. We report the chemical composition of organic fine particulate matter ($PM_{2.5}$), associated emission factors (EFs), and gas-particle phase partitioning for indoor semivolatile organic compounds (SVOCs). Speciated organic $PM_{2.5}$ measurements were made using two-dimensional gas chromatography coupled with high-resolution time-of-flight mass spectrometry (GC×GC-HR-ToF-MS) and semivolatile thermal desorption aerosol gas chromatography (SV-TAG). Organic $PM_{2.5}$ EFs ranged from 7 to 31 mg g^{-1} for burned incense and were largely comprised of polar and oxygenated species, with high abundance of biomass-burning tracers such as levoglucosan. Differences in $PM_{2.5}$ EFs and chemical profiles were observed in relation to the type of incense burned. Nine indoor SVOCs considered to originate from sources other than incense combustion were enhanced during incense events. Time-resolved concentrations of these SVOCs correlated well with $PM_{2.5}$ mass ($R^2 > 0.75$), suggesting that low-volatility SVOCs such as bis(2-ethylhexyl)phthalate and butyl benzyl phthalate partitioned to incense-generated $PM_{2.5}$. Both direct emissions and enhanced partitioning of low-volatility indoor SVOCs to incense-generated $PM_{2.5}$ can influence inhalation exposures during and after indoor incense use.

Keywords: Indoor air, Incense burning, Organics, $PM_{2.5}$, SVOCs, GC×GC, Chemical speciation

Synopsis: Incense particle emissions are chemically similar to organic aerosol from biomass-burning. SVOCs in residential indoor air readily transfer to incense-generated $PM_{2.5}$. Both direct emissions and sorptive partitioning can influence occupant exposures.

Abstract graphic
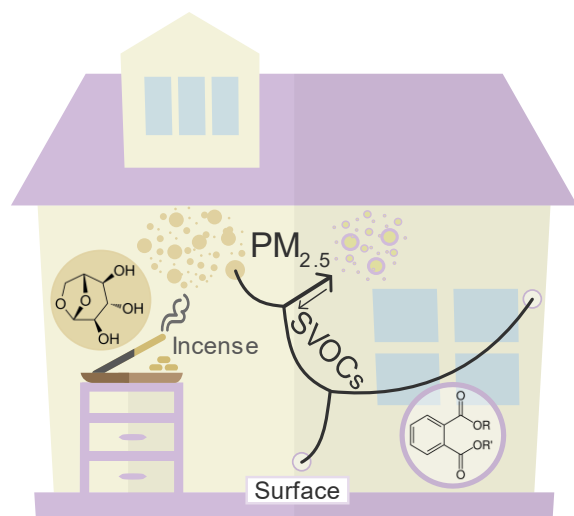
1. INTRODUCTION

Exposure to fine particulate matter (PM$_{2.5}$) is a substantial risk factor for human health.[1] Indoor conditions[2] and air quality can strongly influence one's personal exposure to PM$_{2.5}$ as studies have shown that indoor PM$_{2.5}$ concentrations can sometimes exceed outdoor levels.[3] Given that people spend an average of about two-thirds of their time at home,[4] combined with the health risks associated with PM$_{2.5}$ exposure, it is crucial to improve our understanding of PM$_{2.5}$ indoors. Incense burning is known to be a significant combustion source of residential indoor particulate matter[5,6] with emission factors similar to cigarette smoke.[7] Incense-generated particles are predominantly in the PM$_{2.5}$ size range,[8,9] most concentrated in the accumulation mode,[6,10,11] and characterized by large surface area per unit mass, which allows them to sorb gas-phase organic and inorganic compounds, potentially affecting inhalation exposures.

Incense burning is a traditional practice in many cultures that serves as an integral part of worship and ceremonial functions.[8] Beyond its religious significance, incense serves various other purposes, including therapeutic, aesthetic, insect-repelling, and producing pleasant fragrances.[12] Incense use is most prevalent in the Asia-Pacific, Middle East, and Sub-Saharan African regions, which is reflected in the majority of incense studies and associated adverse health effects emerging prominently from these regions.[8–10,13–20] Incense use is also popular in the West with the US as the largest global importer.[21] While estimates of US domestic incense use are limited, residential settings likely contribute a significant proportion of total incense consumption. Market research shows that incense products saw a surge in popularity and sales during the COVID-19 pandemic, which was driven by demand for enhancing in-home ambiance amid growing mindfulness practices (e.g., meditation and yoga).[22] Despite this increasing trend, incense use remains largely overlooked as a source of indoor PM$_{2.5}$ pollution in Western literature.[23] This oversight is concerning given that a quarter of the US population comprises diverse racial-ethnic and cultural populations whose religions[24] incorporate incense burning into worship practices, potentially influencing household incense use. Furthermore, the religiously unaffiliated, making up another sizable portion of the population, may also frequently burn incense at home for aromatherapy or spiritual reasons, a practice especially common in Black[25] and Latino[26] communities. For instance, one study on polycyclic aromatic hydrocarbons (PAHs) exposure during pregnancy found that 28% of Black and Latino women reported burning incense at home.[27]

Incense-generated PM$_{2.5}$ has been extensively studied indoors with characterization efforts focusing primarily on the physical characteristics of incense emissions, including emission factors, particle mass concentrations, particle size distributions, and particle-associated PAHs in incense smoke.[6,7,11,13–15] Conversely, the speciated chemical composition of incense-generated PM$_{2.5}$ remains largely uncharacterized in indoor environments, despite organic aerosol (OA) constituting the majority of emissions.[8,28–30] Some studies have elucidated the chemical profile of particulate organic matter in incense smoke, particularly from incense sticks, by utilizing chemical characterization techniques such as aerosol mass spectrometry (AMS) and gas chromatography (GC). Yet, such investigations have been restricted to targeted chemical analysis of selected

84   compounds or chemical groups,[16,18,30–32] qualitative explorations of identified species,[33] and
85   organic compositional analysis with low chemical resolution owing to limitations in the speciation
86   capabilities of the instrumentation used.[6,34] Furthermore, these studies have only been conducted
87   in laboratory or controlled environments with some results indicating substantial fractions of OA
88   mass that are unidentified or unresolved.[30,32]

89   Two-dimensional GC coupled with high-resolution mass spectrometry (GC×GC-HR-MS) is a
90   chemical characterization technique that can provide more comprehensive separation and
91   identification of diverse and complex particle-phase organics present in incense smoke.[35] GC×GC
92   has been applied to speciate and quantify thousands of individual chemical species spanning a
93   wide range of volatilities and polarities present in atmospheric matrices.[36,37] Its strengths also lie
94   in separating isomers and several chemically similar compounds that would normally coelute in a
95   one-dimensional GC column. A recent GC×GC-MS laboratory study characterizing total
96   suspended particles from incense emissions could only chemically speciate a small fraction of total
97   particulate organics, owing to quantification challenges that resulted from a lack of chemical
98   derivatization in their analysis approach.[38] When applied to augment a characterization technique
99   like GC×GC, chemical derivatization significantly enhances recovery of polar organic
100   compounds[39] which dominate incense particulate emissions,[33–35,38] and serves to adequately
101   resolve separated compounds in a manner essential for reliable quantification. Employing online
102   chemical derivatization coupled with GC×GC to characterize incense-generated $PM_{2.5}$, as is done
103   in the current work, provides insight into the abundance and behavior of incense-derived particle-
104   phase organics in indoor environments.

105   Assessing air quality impacts of indoor-generated $PM_{2.5}$ requires characterizing common sources.
106   Whereas cooking, candle burning, and smoking have been relatively well studied as indoor
107   combustion sources,[40–42] exploring the chemical composition of incense burning and its
108   contributions to indoor air pollution has been more limited.[43] The current study focuses on
109   evaluating incense $PM_{2.5}$ emissions and the associated chemistry indoors in a normally occupied
110   residence in the San Francisco Bay Area during a period of vacancy. Incense-generated $PM_{2.5}$ was
111   collected on filters for offline organic compositional analysis by GC×GC with supporting
112   semivolatile organic compound (SVOC) measurements using semivolatile thermal-desorption
113   aerosol gas chromatography (SV-TAG). As this work focuses on incense burning indoors, its
114   significance lies in enhancing our understanding of combustion-generated $PM_{2.5}$ in a residential
115   environment, thus offering insights for exposure assessment and source mitigation.

2. METHODS

2.1. Incense Experiments and PM$_{2.5}$ Sample Collection

The analysis explored in this work was conducted in November 2021 during an unoccupied period in an otherwise normally occupied single-family residence in Oakland, California. During incense experiments, the studied home had interior doors open and exterior doors and windows closed. There was no mechanical ventilation and the central air-handling system was off. Detailed descriptions of this H3 field campaign, incense burning protocols, and the rationale behind choosing the study residence and incense scents are provided in the supporting information (SI). Briefly, five incense burning experiments were carried out in H3, each with two sticks of either lavender or Douglas fir incense. Incense burns occurred twice a day around noon and 5:30 pm with incense sticks ignited in the kitchen and allowed to burn through a ~60-min duration before removing the incense source from the residence (see Figure S1 for an illustration of experimental timing). Indoor incense filter samples were collected in the kitchen over 6-h periods on average, along with three outdoor filters simultaneously sampled in the back yard of the H3 residence during incense experiments. Incense smoke was sampled at 10 L min^{-1} on 47 mm quartz filters using a custom-designed aerosol sampler[37] fitted with a cyclone to exclude particles larger than 2.5 µm. Before incense experiments, an indoor air background sample was collected in the kitchen over a 22-h period under closed-home conditions. The H3 occupants reported never burning incense in this residence; thus, the background sample is assumed to be representative of the H3 indoor environment, unperturbed by chemicals related to incense combustion. All H3 samples were collected on heat-treated quartz filters and were stored frozen (-20 °C) prior to chemical analysis.

2.2. PM$_{2.5}$ Filter Analysis: GC×GC

H3 PM$_{2.5}$ filters were analyzed by offline thermal desorption two-dimensional gas chromatography with online derivatization coupled with electron ionization high-resolution time-of-flight mass spectrometry (TD-GC×GC-EI-HR-ToF-MS). A detailed description of instrument methods and specifications as well as quantification, uncertainties, and compositional analysis of H3 samples can be found in the SI (Table S1-S4). Briefly, filter punches (0.07-0.82 cm^2) from H3 samples were initially heated in the instrument's thermal desorption unit under continuous helium gas flow saturated with a derivatization agent, N-methyl-N-(trimethylsilyl)trifluoroacetamide. Desorbed organics were then separated by volatility and polarity, in sequence, by two serially connected GC columns separated by a thermal modulator followed by subsequent ionization under 70 eV EI and detection by HR-ToF-MS with a resolution of 4000. Analyzed PM$_{2.5}$ organics spanned between C$_{13}$ and C$_{36}$ n-alkane volatility equivalents. GC×GC chromatograms were analyzed using the GC Image software and quantification of detected compounds was performed using 110 external standards. Compounds were identified and classified into chemical families through matches with authentic external standards, searches against mass spectral libraries (e.g., NIST-20) utilizing linear retention index (RI), and analysis of second dimension retention times (RT2) and specific molecular ions indicating chemical functionality. Henceforth, chemically "speciated" PM$_{2.5}$ mass concentrations reported and discussed throughout the text are based on H3 filter samples analyzed by GC×GC unless otherwise stated.

## 2.3. Differentiating Indoor and Incense-Attributed Compounds in Incense Samples

The indoor air background sample allowed differentiation between existing conditions at H3 and distinct new compounds observed following incense burns. Compounds detected in the indoor background sample were assigned to a template in GC Image that could be searched against and compared to samples with incense PM$_{2.5}$, through location in GC×GC space (RI and RT2) and EI mass spectra information. In this way, ubiquitous indoor SVOCs such as phthalate ester plasticizers[44,45] along with other compounds identified in the indoor background were characterized as particulate organics not (directly) related to incense combustion, despite their detection in samples collected during incense burning events. Some compounds present in the indoor background air at H3 increased substantially during incense experiments and were likely emitted in incense smoke while other species such as indoor SVOCs may be significantly influenced by incense-generated particle mass as a result of partitioning that enhances their particle-phase abundance.[42,46–49] Compounds observed in the indoor background and the dynamics of their enhancements are discussed in Section 3.3.

2.4. Supporting Analysis for Incense Experiments

Hourly real-time measurements of combined gas and particle-phase organics (gas-plus-particle) smaller than 2.5 µm were collected using an online semivolatile thermal desorption aerosol gas chromatograph (SV-TAG). A detailed description of SV-TAG (e.g., design, operation, uncertainties) can be found elsewhere.[39,50] SV-TAG separately sampled air from the kitchen and the outdoors with measured SVOC volatilities corresponding roughly to the range C_{14} to C_{35} *n*-alkanes. SV-TAG is a GC-based instrument utilized in prior indoor air chemistry campaigns.[47,51] During the H3 campaign, SV-TAG was housed in a temperature-controlled enclosure in the garage-basement. Real-time PM$_{2.5}$ mass was quantified in the kitchen during incense experiments by a Particles Plus (8306) particle counter. Time-resolved particle number concentrations were measured at 1 Hz in six diameter channels between 0.3 and 25.0 µm and mass concentrations were calculated under a particle density assumption of 1 g cm^{-3}. A Sunset Laboratory Model 5L OCEC instrument coupled with the NIOSH870 thermal protocol was used at the Air Quality Research Center at UC Davis to analyze H3 PM$_{2.5}$ filters, including field blanks, for organic carbon (OC) and elemental carbon (EC) content.

3. RESULTS and DISCUSSION
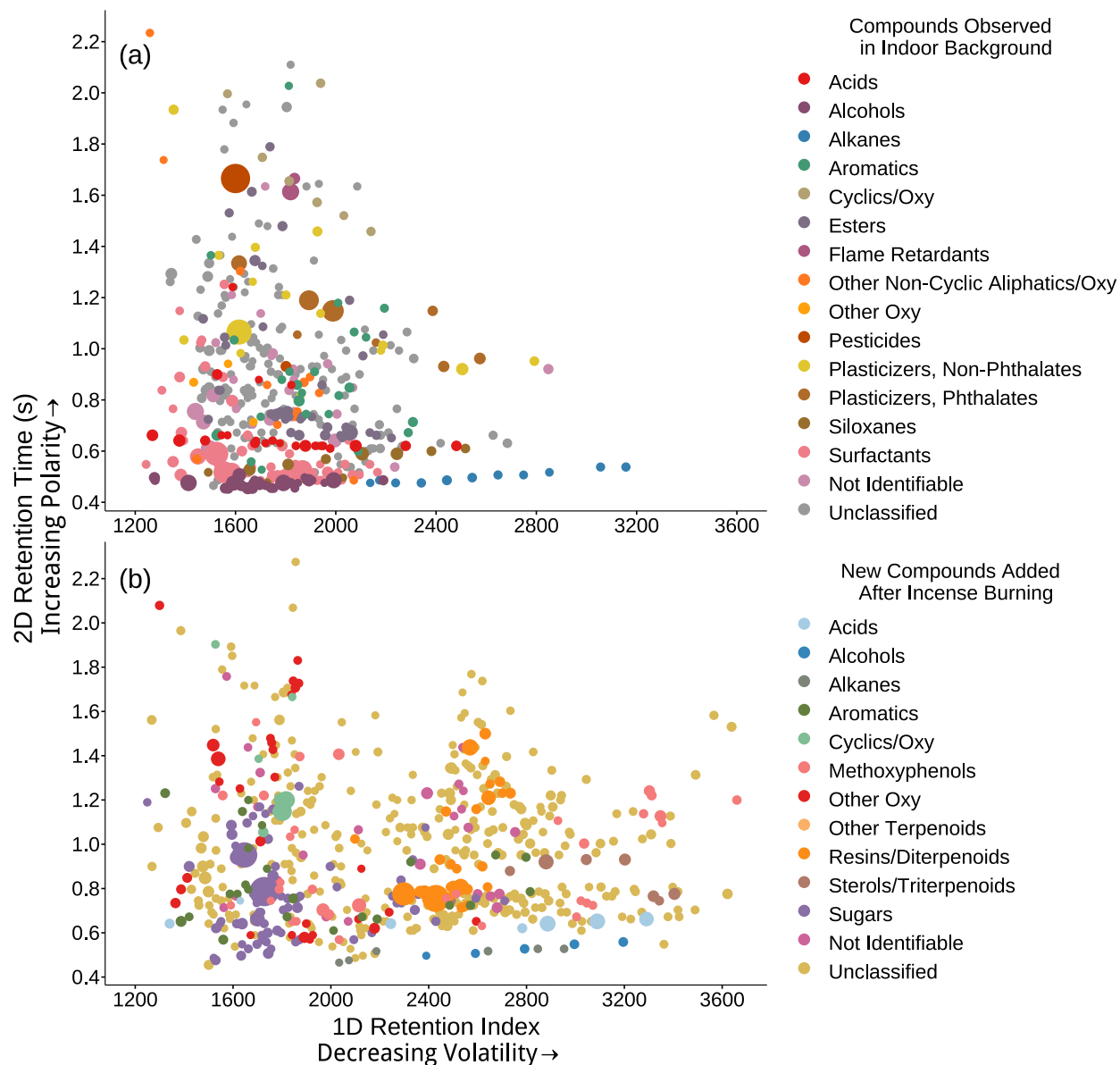
Figure 1. GC×GC chromatograms of (a) the indoor background sample and (b) an incense smoke sample collected from a Douglas fir incense burn event. Compounds are separated by volatility on the *x*-axis and by polarity on the *y*-axis. Each point (panel (a) total = ~460; panel (b) total = 590) corresponds to a unique compound with a full mass spectrum (*m/z* ~35-650). Point size approximately scales with quantified organic aerosol mass concentrations (µg m^{-3}) and colors identify the compound's classification. Differing colors between the same classification (e.g., acids, alcohols, etc.) in both chromatograms highlight indoor background compounds in panel (a) distinct from incense-attributed compounds shown in panel (b) (see Section 2.3).

7

3.1. Chemical Composition of Particulate Organics from Incense Burning

Incense-attributed compounds from both lavender and Douglas fir incense burns exhibited diversity in both structural and chemical properties as shown for a representative incense burn sample in Figure 1b. New compounds following incense burns in H3—i.e., distinct "incense-attributed" compounds not including the indoor background (see Section 2.3)—were distributed over the range of measured species with more compounds inhabiting higher mass (lower volatility) and more oxidized (higher polarity) regions in GC×GC space compared to the indoor background (Figure 1a). Approximately 1600 distinct incense-attributed compounds were separated from incense-generated $PM_{2.5}$ OA samples, of which ~300 compounds were classified into chemical families with 86 of those compounds being positively identified across all five incense burns. The chemical families include acids (carboxylic acids), alcohols, alkanes, aromatics (compounds with at least one aromatic ring), cyclics/oxygenates (non-aromatic/cyclic aliphatics), methoxyphenols, other oxygenates (with two or more -OH groups), other terpenoids (mono- and sesquiterpenoids), resins/diterpenoids, sterols/triterpenoids, and sugars (with sugar derivatives including anhydrosugars and sugar alcohols). Compounds with signal responses above the selected intensity cutoff that could not be identified or classified during analysis were categorized as not identifiable while the remainder of the compounds under this limit were grouped as unclassified.

Incense-attributed compounds were closely related to smoke particles found in biomass-burning organic aerosol (BBOA).[37,52] These findings were consistent with previous studies,[32,34,38] as the composition of incense sticks (e.g., aromatic woods, flowers, resins, etc.) supports the observation of wood pyrolysis products as found in BBOA. The range of observed BBOA compounds demonstrated the elevated presence of polar and oxygenated organic compounds in incense smoke. This finding was confirmed by estimating the incidence of derivatization in GC×GC, which accounted for more than 88% of all incense-attributed compounds across incense burn samples. The process for determining the fraction of separated compounds that were derivatized is discussed in the SI (see Figure S2). Due to the derivatization process used in this work, many polar organics were both recovered and well resolved, making it possible to reliably integrate and quantify these speciated compounds. However, speciated compounds differ chemically from their original forms with derivatization, which can create some challenges for identification and classification as derivatized mass spectra may not be available or published in MS libraries or literature.[37,53] Overall, 29–39% of incense-attributed compounds were classified within each analyzed incense burn sample.
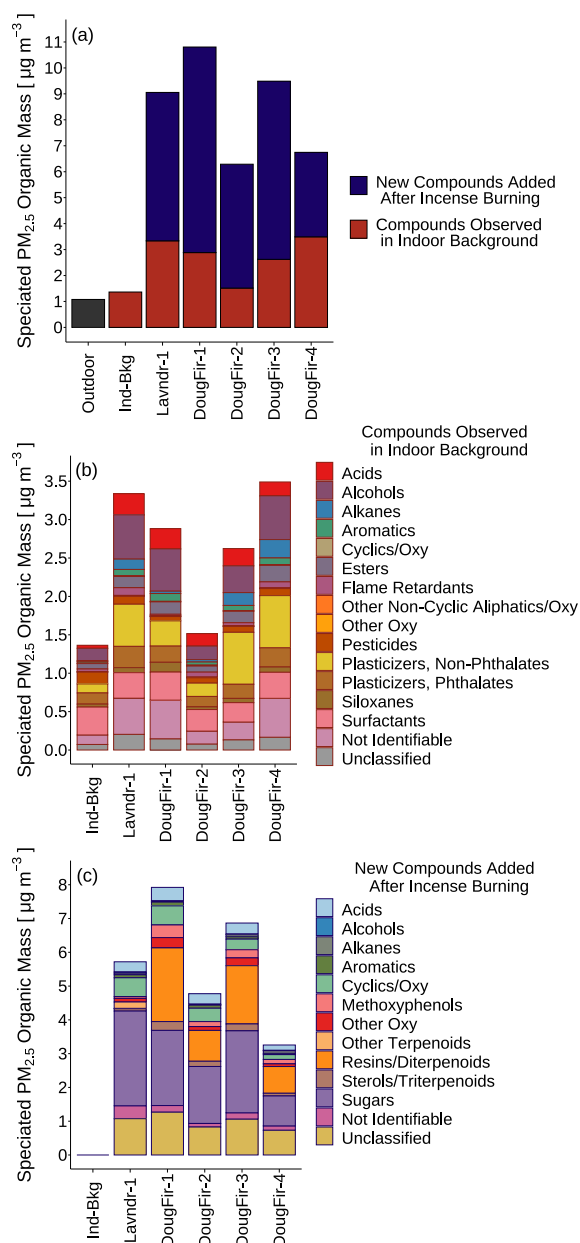
Figure 2. GC×GC speciated PM$_{2.5}$ organic aerosol mass concentrations for (a) total quantified mass in H3 filter samples, with designated mass fractions in incense samples, (b) indoor background mass fractions classified by chemical family in each sample, and (c) incense-attributed mass fractions classified by chemical family in incense samples. Note the different *y*-axis scales in (b) and (c) in contrast to (a), and that the sum of (b) and (c) equals (a) for incense samples. Each stacked bar in (b) and (c) shows the sum of concentrations of classified compounds in each sample (see Table S6 and S7). Colors that differ between common chemical families (e.g., acids, alcohols, etc.) in (b) and (c) highlight that compounds within those chemical families are distinct between indoor background and incense-attributed masses. "Ind-Bkg" refers to the indoor air background sample, "Lavndr" refers to a sample with lavender incense burned, and "DougFir" refers to a sample with Douglas fir incense burned.

3.2. Speciated Organic PM$_{2.5}$ Mass Contributions from Incense Emissions

Total GC×GC speciated PM$_{2.5}$ OA concentrations are shown in Figure 2a for incense samples, with mass fraction contributions from both indoor background and incense-attributed compounds. Incense samples contained mass concentrations 4.6–7.9 times higher than the indoor background. Incense-attributed compounds shown in Figure 1b accounted for 3.3–7.9 µg m^{-3} (48–73%) of total speciated mass in incense samples (Figure 2a). The lower limit of the incense-attributed mass fraction is likely related to incomplete incense combustion for the DougFir-4 sample (see SI). The total outdoor mass concentration, 1.1 µg m^{-3}, is the average of the three outdoor filter samples collected at H3. The incense-attributed mass fraction for each incense sample is summarized by chemical family in Figure 2c. Classified compounds accounted for 74–82% of incense-attributed mass across burns while the not identifiable and unclassified compounds represented on average about a fifth (18–26%). Sugars contributed the highest proportion (27–49%) to incense-attributed mass for all burns with levoglucosan, an unequivocal BBOA tracer, being the most abundant sugar compound emitted (41–62%). Levoglucosan was also the highest mass contributor across all incense-attributed compounds with concentrations ranging from 0.4 to 1.3 µg m^{-3}. This finding aligns with reported high levoglucosan emissions from incense burning[38] and as pyrolysis products of primarily cellulose-rich plant materials[54] such as those used in producing incense. Other important BBOA tracers such as resins/diterpenoids were also abundant (19–28%) in Douglas fir burn samples as the second highest contributing incense-attributed chemical family. These compounds are indicative of conifer species[37,55–57] such as the Douglas fir incense burned in H3. Emissions of dehydroabietic acid, which is an identified marker of conifer combustion,[56] was also in agreement with BBOA studies[56,57] as the most abundant resin/diterpenoid (27–33%) with speciated mass concentrations of 0.2–0.7 µg m^{-3} for the four Douglas fir burn samples. Palustric acid was the second highest mass contributor of the resins/diterpenoids chemical family (17–26%) in Douglas fir samples with concentrations of 0.1–0.5 µg m^{-3}. This compound is distinct to pine species[37,55] and likely originated from the addition of "piñon pine" highlighted in the list of ingredients for Douglas fir incense.

For the single burn sample of lavender incense (non-conifer), resins/diterpenoids only made up 0.2% of the incense-attributed mass with a concentration < 0.01 µg m^{-3}. Furthermore, only the lavender burn exhibited other terpenoid compounds such as mono- and sesquiterpenoids. These compounds accounted for 3.3% of incense-attributed speciated mass and are distinctive to fragrant plants like lavender. Also, compared to Douglas fir samples, lavender incense emitted much less mass of methoxyphenols (3.1–4.7% vs 0.9%). Since methoxyphenols are pyrolysis products of lignin and indicative of burned wood in fine aerosol,[56] this difference is likely a result of more woody biomass components being present in Douglas fir incense compared to the higher floral content used in producing lavender incense. These variations in the organic chemical composition of incense-generated PM$_{2.5}$ are likely influenced by components of the incense materials used,[10,38] and are relevant given that the toxicity of BBOA, and incense by proxy, depends partly on chemical composition.[58] The vast majority of these compounds have unknown health impacts;[52] nonetheless, some BBOA-related compounds with hazard codes outlined in the SI of Liang et al.[52] were

279 positively identified in this work as summarized in Table S5. Additional BBOA-related chemical
280 families contributing to incense-attributed mass fractions in Figure 2c are provided in Table S6.

281 In this study, PAHs were not detected in $PM_{2.5}$ organic aerosol collected on incense filter samples
282 analyzed by GC×GC, including lower volatility PAHs with four rings or more (e.g., fluoranthene),
283 which are generally found in the particle phase.[59] This observation was surprising given the
284 prominent role of PAHs as products of incomplete combustion of carbonaceous fuels as is
285 characteristic of incense burning. While some studies have explored particle-associated PAHs in
286 incense emissions,[13,14,16] others have encountered challenges in measuring these compounds
287 indoors, such as in Lung et al.[15] who estimated household incense PAHs emissions through
288 laboratory combustion.[60] Observed mass loadings of PAHs from their laboratory experiments were
289 less than 0.1% of total particle mass, with similar ratios reported in later studies in a controlled
290 experimental house[6] and during chamber combustion.[16] Yang et al.[16] reported that emission factors
291 of gas-phase PAHs were about three times higher than particle-associated PAHs and Lin et al.[14]
292 found that 90% of indoor airborne PAHs from incense burning were in the gas phase. These studies
293 suggest that open combustion indoors, incense composition, particle loading, and PAH abundance
294 in the gas phase may have impeded detection of particle-bound PAHs in H3 incense samples.

3.3. Influence of Incense Burning on Indoor Compounds and SVOCs Concentrations

297 The speciated chemical composition of compounds observed in the indoor background sample is
298 depicted in Figure 1a. Approximately 460 background compounds observed in H3 were largely
299 concentrated within more volatile regions (95th percentile RI < C_{24}) in GC×GC space compared to
300 compounds attributed to incense in Figure 1b. This finding indicates that indoor background
301 compounds were predominantly higher volatility SVOCs species such as plasticizers (e.g., from
302 floor coverings and personal care products) and surfactants (e.g., in detergents and cleaners), which
303 are abundant and persist in indoor air from stable or recurring indoor sources.[44] Analysis of the
304 indoor background sample resulted in 58% of observed compounds classified into broad chemical
305 families: esters, flame retardants, other non-cyclic aliphatics/oxygenates, pesticides, plasticizers
306 (non-phthalates and phthalates), and surfactants (non-ionic, alcohol ethoxylates). Chemical
307 families of indoor background compounds matching those illustrated in Figure 1b for incense are
308 described in Section 3.1. Compounds observed in the indoor background sample had a total mass
309 concentration of 1.4 µg m^{-3} (Figure 2a) and accounted for 1.5–3.5 µg m^{-3} (24–52%) of total
310 speciated mass in incense samples. Figure 2b displays the speciated mass concentrations of
311 chemical families, describing the range of observed indoor background compounds and their
312 abundance with respect to incense samples (Table S7). Classified compounds accounted for 75–
313 86% of the indoor background mass fraction across all samples shown in Figure 2b. For indoor
314 background compounds detected in incense samples, we treated the indoor air background sample
315 as the baseline for these non-incense-attributed compounds. This approach allows for broad
316 observations of changes in the abundance and enhancements of indoor background compounds
317 across incense samples.

Using GC×GC speciated mass, enhancement ratios (ERs) were calculated from the increases in the time-averaged concentrations of indoor background compounds detected in incense samples relative to (i.e., divided by) the indoor background sample. In this study, ERs for a given compound had to be consistently greater than two (2) across all incense samples to be considered "enhanced". Additionally, compounds detected in incense samples that were completely absent from the indoor background sample were manually searched at levels below normal analytical limits of detection (LOD) in the background sample to ensure that they were not misattributed due to changes in LOD from differing sampling volumes. Figure 3 illustrates the range of ERs calculated for indoor background compounds detected in the DougFir-1 incense sample. Table S8 reports all indoor background compounds that were consistently enhanced across incense samples and were positively identified. Background indoor compounds within acid, alkane, alcohol, aromatic, ester, and plasticizer chemical families were found to be consistently enhanced across incense samples, with variability in ER values. The enhancements of acids, alcohols, and alkanes most likely relate to direct OA emissions from incense burns. Observed background compounds such as C_{20} acid (eicosanoic acid) and C_{27} alkane (heptacosane) were previously shown to be constituents of primary BBOA, emitted abundantly in samples collected during wildfires.[52] This evidence is consistent with high mean and median ERs for eicosanoic acid (14.5 and 16.0) and heptacosane (46.5 and 42.8) in incense samples. Both eicosanoic acid and heptacosane as well as other enhanced indoor background acids, alkanes, and alcohols have been previously reported in incense emissions.[35,38]
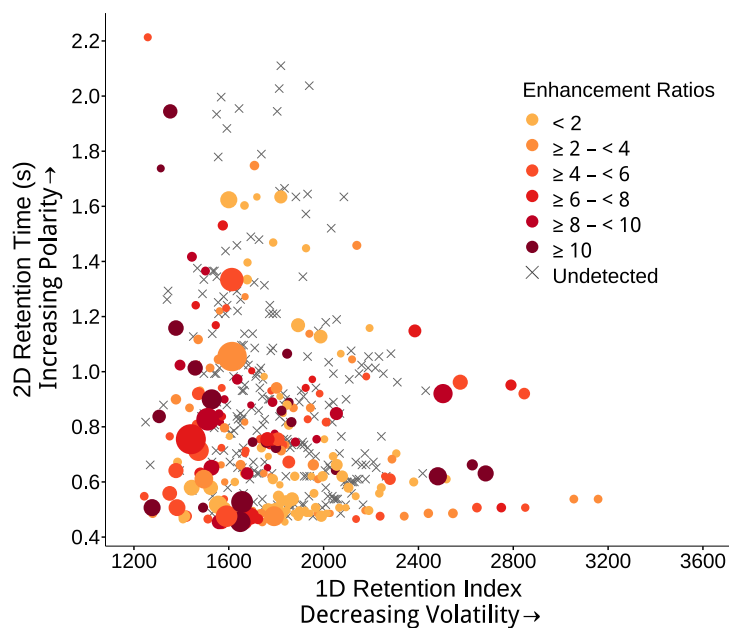
Figure 3. Enhancement ratios of indoor background compounds detected in DougFir-1 incense sample. Point size indicates the quantified organic aerosol mass concentration (µg m^{-3}) in GC×GC, and the color scale identifies the enhancement ratio compared to the indoor background sample. "Undetected" refers to indoor background compounds not detected in DougFir-1.

343 The enhanced aromatic, ester, and plasticizer compounds we observed in incense samples were
344 mostly SVOC species related to building materials and consumer items such as personal care
345 products. For example, homosalate is an SVOC used in the production of sunscreen,[61] which has
346 been found in residential indoor air during occupancy independent of cooking or cleaning
347 activities.[51] Isopropyl myristate, commonly used as a cosmetic ingredient in personal care
348 products, was detected in 100% of household dust samples collected in a study in northern
349 California.[62] Bis(2-ethylhexyl) phthalate (DEHP) and butyl benzyl phthalate (BBzP) are widely
350 used as plasticizers that make up large mass fractions of several construction and furnishing
351 materials.[63] They have also been measured extensively in residential indoor environments.[64]
352 Diethyl phthalate (DEP) is an abundant plasticizer present in furnishings as well as in personal
353 care products.[63] Bis(2-ethylhexyl) terephthalate (DEHT) is a high production volume non-
354 phthalate plasticizer, often used as a replacement for DEHP, in consumer products and building
355 materials.[65] 2,2,4-Trimethyl-1,3-pentanediol diisobutyrate (trade name TXIB; Eastman Chemical)
356 is another non-phthalate plasticizer that is used largely in vinyl products such as flooring and wall
357 coverings.[66] TXIB, DEP, and isopropyl myristate were also shown in one study to dominate SVOC
358 peak abundances in residential indoor air under closed conditions prior to window opening.[67] To
359 better understand the dynamic behavior of these assumed indoor originating SVOCs detected and
360 enhanced in incense filter samples, we provide relative abundances of gas-plus-particle samples
361 of these compounds during incense burns using SV-TAG.

3.4. Influence of Incense-Generated PM$_{2.5}$ on Gas- and Particle-Phase Partitioning of Indoor SVOCs

364 Nine indoor SVOCs were compared to particle mass at hourly resolution during incense burning
365 events using the SV-TAG and Particles Plus instruments respectively (Figure 4). The first four
366 compounds in the top and bottom panels in Figure 4 represent SVOCs with volatilities above and
367 below C$_{23}$ alkane-equivalent volatility respectively. This distinction is highlighted to explain
368 dynamic SVOC behavior that has been reported in prior residential indoor air studies. Using the
369 same instrument and methods in an observational study, Lunderberg et al.[47] reported that certain
370 indoor SVOCs exhibited shifting gas-particle phase partitioning in response to changes in PM$_{2.5}$
371 concentration. SVOCs with volatilities lower than the C$_{23}$ alkane were observed to partition onto
372 airborne particles when particle mass concentration increased. This effect was less prominent for
373 higher volatility SVOCs. We observed similar effects in our experimental incense study with the
374 strongest correlations for SVOCs with lower volatilities (Figure 4). For SV-TAG samples of
375 indoor SVOCs with volatilities above C$_{23}$, the background concentrations were mostly gaseous as
376 evidenced by the high intercepts of the regression lines for gas-plus-particle measurements shown
377 in Figure 4. With increased PM$_{2.5}$ mass during incense burning events, concentrations of these
378 higher volatility SVOCs generally remained above background levels. Similar behavior was
379 reported by Lunderberg et al.[47] and Kristensen et al.[46] as these higher volatility indoor SVOCs
380 were not expected to strongly partition to airborne PM$_{2.5}$. In contrast, for indoor SVOCs below C$_{23}$
381 volatility, as displayed in the bottom panel of Figure 4, strong associations between total (gas-plus-
382 particle) SVOC abundance and incense particle mass concentrations were observed, with

383 regression intercepts close to zero across displayed compounds. These relationships strengthen
384 moving from left to right for these lower volatility SVOCs, as partitioning to airborne particles
385 appears to drive the enhancement of their airborne particle-phase concentrations.

386 Some laboratory incense chamber studies have shown the presence of certain plasticizers and
387 related indoor SVOCs in particulate incense emissions.[31,38] DEP is the only phthalate plasticizer
388 that has been reported to be used as a binder ingredient for incense production in India.[17,68] In the
389 present work, although DEP was enhanced in incense filter samples, there was no real-time
390 association with airborne particles during incense burning experiments (Figure 4) when compared
391 to similar higher volatility indoor SVOCs. For other plasticizers and SVOCs discussed, the gas-
392 particle phase partitioning behavior presented in this work, and supported by SVOC measurements
393 in prior indoor studies, provides substantial evidence that these SVOCs largely originate from
394 other residential indoor sources, rather than directly from incense emissions. Furthermore, if it
395 were the case that the discussed indoor SVOCs were emitted primarily from incense emissions,
396 one would expect to observe different time-resolved behavior of their abundance in indoor air than
397 was exhibited in the SV-TAG data. Specifically, associations should be very strongly correlated
398 with incense-generated $PM_{2.5}$ as the increases and eventual decay of airborne $PM_{2.5}$ would be equal
399 to the presence and relative abundance of emitted indoor SVOCs.

400 Overall, the findings in this work are consistent with prior studies in residences[46,47] and
401 chambers,[69] augmented by modeling studies,[70] which specifically show enhanced DEHP emissions
402 from surfaces being influenced by the presence of airborne particles. That lower volatility SVOCs
403 sorb to incense-generated particles is important for recognizing how SVOCs can indirectly
404 contribute to indoor organic $PM_{2.5}$ mass and how strong indoor particle sources can alter the mode
405 and intensity of SVOC inhalation exposures for occupants.[44] Inhaled $PM_{2.5}$ with increased toxicity
406 from sorbed SVOCs would deposit in the respiratory tract differently than would a gas-phase
407 SVOC.[71] These observations are not only relevant for indoor SVOCs such as DEHP and BBzP,
408 which have been shown to contribute to adverse health outcomes in their roles as endocrine-
409 disrupting chemicals,[72] but also for other unexplored low-volatility indoor SVOCs with unknown
410 health effects.
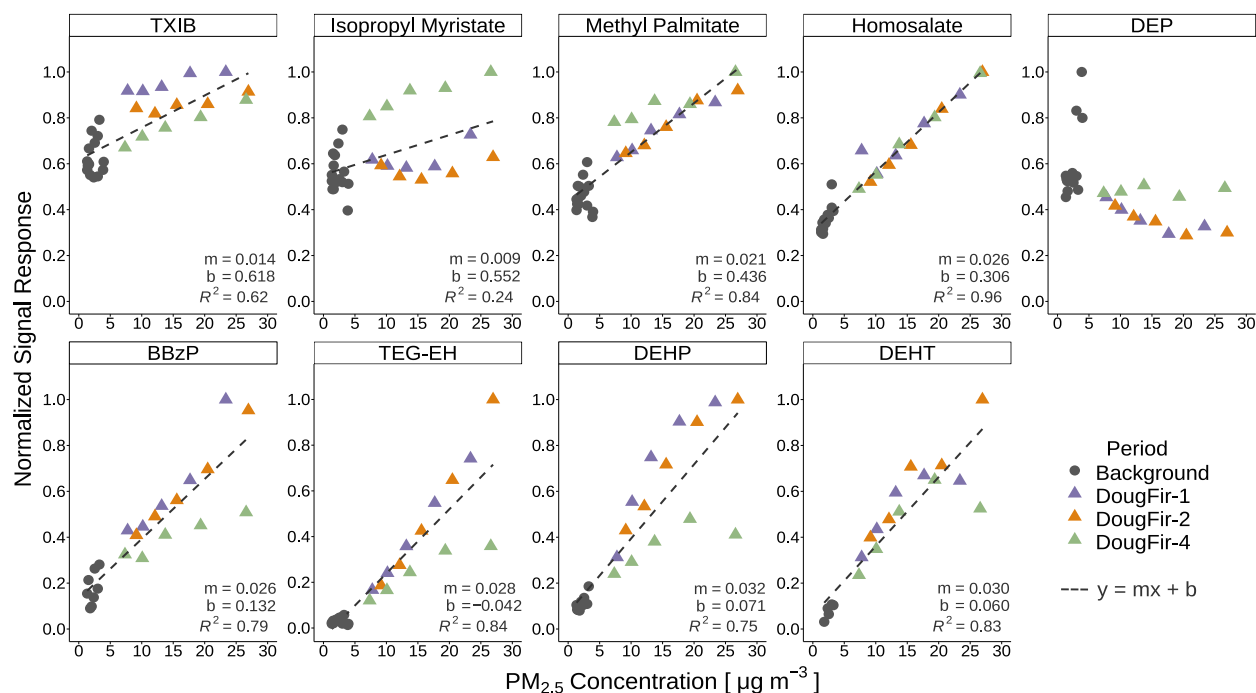
Figure 4. Associations of time-resolved indoor SVOCs abundance with $PM_{2.5}$ mass concentrations during incense burning experiments. Reported SVOC measurements are total (gas-plus-particle) internal standard normalized signal (equivalent to mass concentrations). SVOCs are arranged in order of increasing retention index (see Table S8). "TXIB," "DEP," "BBzP," "TEG-EH," "DEHP," and "DEHT" refer to 2,2,4-trimethyl-1,3-pentanediol diisobutyrate, diethyl phthalate, butyl benzyl phthalate, triethylene glycol di(2-ethylhexoate), bis(2-ethylhexyl) phthalate, and bis(2-ethylhexyl) terephthalate, respectively.

3.5. Emission Factors of Incense-Generated $PM_{2.5}$ in Indoor Air

Consistent with prior incense studies,[28,29] total organic carbon (OC) mass comprised the majority of $PM_{2.5}$ in incense filter samples with concentrations of 17.4–37.2 µg m^{-3}. An assumed OA/OC ratio of 1.6, as derived from field and laboratory primary BBOA AMS measurements,[73,74] was applied to estimate total $PM_{2.5}$ OA in incense samples based on OC measurements (Table S9). The speciated mass concentrations of indoor background and incense-attributed compounds quantified in incense samples (Figure 2a) can explain, on average, 20% of the total $PM_{2.5}$ OA mass in each sample. This extent of successful speciation is credited to online derivatization that facilitated enhanced recovery of more polar and oxygenated incense particle-phase organics compared to non-derivatized analysis of incense emissions.[38]

To evaluate and more easily compare incense burning contributions in H3 with prior studies, $PM_{2.5}$ emission factors (mass of $PM_{2.5}$ emitted per mass of incense burned) were estimated using the integral mass balance approach for episodic emissions.[75] Equation (1) determines the mass, M, of $PM_{2.5}$ emitted from an incense burn event in a well-mixed indoor environment with volume, V, where C_i is the time-averaged OA concentration in incense filter samples, C_b is the background OA concentration in H3, Δt is the sampling duration, and L is the total removal rate of incense-

15

435 generated PM$_{2.5}$ during and following emissions. L was estimated by fitting time-resolved incense
436 PM$_{2.5}$ data from the Particles Plus to a first-order decay[76] (see SI). For this calculation, a few
437 assumptions were made: 1) incense-generated PM$_{2.5}$ is well-mixed throughout the interior volume
438 of H3 during the burning and decay period; 2) the background OA concentration during incense
439 burns is the same as that measured in the time-averaged indoor background sample collected prior
440 to incense experiments; and 3) the loss rate estimated during the post-burning decay period applies
441 throughout the incense emission event. Applying these assumptions, the PM$_{2.5}$ emission factor,
442 EF, is then estimated using equation (2), where m is the mass of two incense sticks burned per
443 experiment.

444 $$M = V \cdot L \cdot (C_i - C_b) \cdot \Delta t \quad eq\ (1)$$

445 $$EF = \frac{M}{m} \quad eq\ (2)$$

446 Evidence from analysis of episodic point source emissions[77] shows that the use of the well-mixed
447 assumption should not result in large estimation errors if the gamma (γ; source inactive and well
448 mixed) period is longer than the alpha (α; source active and poorly mixed) plus beta (β; source
449 inactive and poorly mixed) periods. Figure S3 illustrates time-resolved PM$_{2.5}$ concentrations for
450 one of the experimental runs, showing that the duration of alpha plus beta periods is much less
451 than the gamma period. PM$_{2.5}$ EFs from incense experiments ranged from 7 to 31 mg g^{-1} (Table
452 S10) and were within the range of results from other incense stick burning studies[9,12,16,29,59]
453 summarized in Table S11. Estimated PM$_{2.5}$ EFs in this work indicated that Douglas fir incense
454 burns (average: 27 mg g^{-1}) produced more PM$_{2.5}$ emissions than lavender (7 mg g^{-1}), which is
455 likely attributable to higher carbonaceous matter from woody biomass materials in Douglas fir
456 incense compared to the higher floral content in lavender incense. The estimated EFs could be
457 affected by both incense composition and burning conditions, which can vary in ways that are
458 neither easily predicted nor effectively controlled in H3 incense experiments. Nonetheless, results
459 suggest that the severity of indoor particle pollution from incense burning may be influenced by
460 incense scent or materials. In particular, incense with lower carbon and higher calcium content has
461 been shown to result in lower particle emission factors.[16,78] Incense burning is often an episodic or
462 short-term source of PM$_{2.5}$ indoors; however, long-term habitual use by occupants could have
463 cumulative effects on indoor air pollution and human health.

3.6. Implications

465 Exposure to incense-generated PM$_{2.5}$ has been shown to be harmful to human health.[20] In this
466 study, we characterized in detail the chemical profile of fine particulate matter resulting from five
467 incense burning experiments in the H3 residence. Organic PM$_{2.5}$ fractions from lavender and
468 Douglas fir incense burns resulted in 4.6–7.9 times higher concentrations of speciated OA
469 compared to background conditions when averaged over 6-h time periods. Incense-attributed
470 compounds showed clear similarities to BBOA with abundant masses of tracers such as
471 levoglucosan and dehydroabietic acid. Incense type also influenced the chemical composition of
472 OA as well as EFs with Douglas fir incense generating more PM$_{2.5}$ than lavender (27 vs 7 mg g^{-1}).

Furthermore, ubiquitous indoor SVOCs, such as plasticizers, observed in H3 indoor background air were influenced by increasing $PM_{2.5}$ concentrations during incense burns due to volatility-dependent gas-particle phase partitioning. Low-volatility indoor SVOCs were shown to strongly correlate ($R^2 > 0.75$) with time-resolved concentrations of $PM_{2.5}$ mass during incense burning events, thus indirectly contributing to organic $PM_{2.5}$ incense mass. These observations also demonstrate how the chemical composition of incense-generated $PM_{2.5}$ can be altered in indoor air and point to potential increases in occupant uptake of low-volatility SVOCs such as DEHP and BBzP, through shifts in their airborne concentrations and gas-particle phase partitioning. We showed that incense burning, when it occurs, is a substantial combustion source of indoor $PM_{2.5}$ pollution with diverse chemical complexity and interactions with components of the indoor environment. As such, more research directed toward chemical speciation would help to better understand the impacts of incense burning emissions on indoor air quality in different indoor environments. Given that this study was conducted in a single residence with only two types of incense tested, readers are advised to exercise caution in extrapolating toward generalized conclusions from this study.

AUTHOR CONTRIBUTIONS

J.O. wrote the manuscript, conducted incense experiments, and analyzed H3 $PM_{2.5}$ filter samples; M.R.A., Y.L., and E.B.F. supported data analysis and manuscript development; D.M.L. collected and analyzed SV-TAG SVOCs data; C.E.I. supported experimental design and manuscript development; B.C.S., W.W.N., and A.H.G. oversaw incense experiments and sample and data analysis. All co-authors reviewed and contributed comments to the manuscript.

SUPPORTING INFORMATION

GC×GC methods and materials, quantification, compositional analysis, and derivatization; Detailed descriptions of field campaign and incense experiments; Speciated mass concentrations of indoor background and incense-attributed chemical families in incense $PM_{2.5}$ samples; Enhancement ratios of indoor background compounds; Incense $PM_{2.5}$ OC, OA, loss rates, and EFs.

ACKNOWLEDGMENTS

AUTHOR INFORMATION

Corresponding Author

Jennifer Ofodile – *Department of Environmental Science, Policy, and Management, University of California, Berkeley, Berkeley, CA 94720, United States*

Authors

Michael R. Alves – *Department of Environmental Science, Policy, and Management, University of California, Berkeley, Berkeley, CA 94720, United States*

Yutong Liang – *Department of Environmental Science, Policy, and Management, University of California, Berkeley, Berkeley, CA 94720, United States; Now at School of Chemical and Biomolecular Engineering, Georgia Institute of Technology, Atlanta, GA 30332, United States*

Emily B. Franklin – *Department of Civil and Environmental Engineering, University of California, Berkeley, Berkeley, CA 94720, United States; Now at Environment Unit, CSIRO, Aspendale, 3195, Australia*

David M. Lunderberg – *Department of Environmental Science, Policy, and Management, University of California, Berkeley, Berkeley, CA 94720, United States; Now at Office of Energy Efficiency & Renewable Energy, AAAS Science, Technology and Policy Fellow, U.S. Department of Energy, Washington, DC 20585, United States*

Cesunica E. Ivey – *Department of Civil and Environmental Engineering, University of California, Berkeley, Berkeley, CA 94720, United States*

Brett C. Singer – *Indoor Environment Group, Energy Analysis and Environmental Impacts Division, Building Technologies and Urban Systems Division, Energy Technologies Area, Lawrence Berkeley National Laboratory, Berkeley, CA 94720, United States*

William W Nazaroff – *Department of Civil and Environmental Engineering, University of California, Berkeley, Berkeley, CA 94720, United States*

Allen H. Goldstein – *Department of Environmental Science, Policy, and Management, University of California, Berkeley, Berkeley, CA 94720, United States; Department of Civil and Environmental Engineering, University of California, Berkeley, Berkeley, CA 94720, United States*

REFERENCES

(1) GBD 2019 Risk Factors Collaborators. Global burden of 87 risk factors in 204 countries and territories, 1990–2019: a systematic analysis for the Global Burden of Disease Study 2019. *The Lancet* **2020**, 396, 1223–1249. https://doi.org/10.1016/S0140-6736(20)30752-2.

(2) Goldstein, A. H.; Nazaroff, W. W.; Weschler, C. J.; Williams, J. How Do Indoor Environments Affect Air Pollution Exposure? *Environmental Science & Technology* **2021**, *55*, 100–108. https://doi.org/10.1021/acs.est.0c05727.

(3) Mannan, M.; Al-Ghamdi, S. G. Indoor Air Quality in Buildings: A Comprehensive Review on the Factors Influencing Air Pollution in Residential and Commercial Structure. *International Journal of Environmental Research and Public Health* **2021**, *18*, 3276. https://doi.org/10.3390/ijerph18063276.

(4) Klepeis, N. E.; Nelson, W. C.; Ott, W. R.; Robinson, J. P.; Tsang, A. M.; Switzer, P.; Behar, J. V.; Hern, S. C.; Engelmann, W. H. The National Human Activity Pattern Survey (NHAPS): a resource for assessing exposure to environmental pollutants. *Journal of Exposure Science & Environmental Epidemiology* **2001**, *11*, 231–252. https://doi.org/10.1038/sj.jea.7500165.

(5) Apte, K.; Salvi, S. Household air pollution and its effects on health. *F1000Research* **2016**, *5*, F1000 Faculty Rev-2593. https://doi.org/10.12688/f1000research.7552.1.

(6) Ji, X.; Le Bihan, O.; Ramalho, O.; Mandin, C.; D'Anna, B.; Martinon, L.; Nicolas, M.; Bard, D.; Pairon, J.-C. Characterization of particles emitted by incense burning in an experimental house. *Indoor Air* **2010**, *20*, 147–158. https://doi.org/10.1111/j.1600-0668.2009.00634.x.

(7) Mannix, R. C.; Nguyen, K. P.; Tan, E. W.; Ho, E. E.; Phalen, R. F. Physical characterization of incense aerosols. *Science of The Total Environment* **1996**, *193*, 149–158. https://doi.org/10.1016/S0048-9697(96)05343-0.

(8) Wang, B.; Lee, S. C.; Ho, K. F.; Kang, Y. M. Characteristics of emissions of air pollutants from burning of incense in temples, Hong Kong. *Science of The Total Environment* **2007**, *377*, 52–60. https://doi.org/10.1016/j.scitotenv.2007.01.099.

(9) Lee, S.-C.; Wang, B. Characteristics of emissions of air pollutants from burning of incense in a large environmental chamber. *Atmospheric Environment* **2004**, *38*, 941–951. https://doi.org/10.1016/j.atmosenv.2003.11.002.

(10) Chang, Y.-C.; Lee, H.-W.; Tseng, H.-H. The formation of incense smoke. *Journal of Aerosol Science* **2007**, *38*, 39–51. https://doi.org/10.1016/j.jaerosci.2006.09.003.

(11) Cheng, Y. S.; Bechtold, W. E.; Yu, C. C.; Hung, I. F. Incense Smoke: Characterization and Dynamics in Indoor Environments. *Aerosol Science and Technology* **1995**, *23*, 271–281. https://doi.org/10.1080/02786829508965312.

(12) Jetter, J. J.; Guo, Z.; McBrian, J. A.; Flynn, M. R. Characterization of emissions from burning incense. *Science of The Total Environment* **2002**, *295*, 51–67. https://doi.org/10.1016/S0048-9697(02)00043-8.

(13) Li, C.-S.; Ro, Y.-S. Indoor characteristics of polycyclic aromatic hydrocarbons in the urban atmosphere of Taipei. *Atmospheric Environment* **2000**, *34*, 611–620. https://doi.org/10.1016/S1352-2310(99)00171-5.

(14) Lin, T.-C.; Chang, F.-H.; Hsieh, J.-H.; Chao, H.-R.; Chao, M.-R. Characteristics of polycyclic aromatic hydrocarbons and total suspended particulate in indoor and outdoor atmosphere of a Taiwanese temple. *Journal of Hazardous Materials* **2002**, *95*, 1–12. https://doi.org/10.1016/S0304-3894(02)00146-2.

(15) Lung, S.-C. C.; Kao, M.-C.; Hu, S.-C. Contribution of incense burning to indoor PM_{10} and particle-bound polycyclic aromatic hydrocarbons under two ventilation conditions. *Indoor Air* **2003**, *13*, 194–199. https://doi.org/10.1034/j.1600-0668.2003.00197.x.

(16) Yang, C.-R.; Lin, T.-C.; Chang, F.-H. Particle size distribution and PAH concentrations of incense smoke in a combustion chamber. *Environmental Pollution* **2007**, *145*, 606–615. https://doi.org/10.1016/j.envpol.2005.10.036.

(17) Lin, T.-C.; Krishnaswamy, G.; Chi, D. S. Incense smoke: clinical, structural and molecular effects on airway disease. *Clinical and Molecular Allergy* **2008**, *6*, 3. https://doi.org/10.1186/1476-7961-6-3.

(18) Bootdee, S.; Chantara, S.; Prapamontol, T. Determination of $PM_{2.5}$ and polycyclic aromatic hydrocarbons from incense burning emission at shrine for health risk assessment. *Atmospheric Pollution Research* **2016**, *7*, 680–689. https://doi.org/10.1016/j.apr.2016.03.002.

(19) Cohen, R.; Sexton, K. G.; Yeatts, K. B. Hazard assessment of United Arab Emirates (UAE) incense smoke. *Science of The Total Environment* **2013**, *458–460*, 176–186. https://doi.org/10.1016/j.scitotenv.2013.03.101.

(20) Wong, A.; Lou, W.; Ho, K.; Yiu, B. K.; Lin, S.; Chu, W. C.; Abrigo, J.; Lee, D.; Lam, B. Y.; Au, L. W.; Soo, Y. O.; Lau, A. Y.; Kwok, T. C.; Leung, T. W.; Lam, L. C.; Ho, K.; Mok, V. C. Indoor incense burning impacts cognitive functions and brain functional connectivity in community older adults. *Scientific Reports* **2020**, *10*, 7090. https://doi.org/10.1038/s41598-020-63568-6.

(21) Knight, L.; Levin, A.; Mendenhall, C. *Candles and incense as potential sources of indoor air pollution: market analysis and literature review*. Report No. EPA-600/R-01-001 (NTISPB2001-103924); US Environmental Protection Agency, 2001. https://www.epa.gov/nscep.

(22) Watters, R. *Aircare US, 2022: Aircare Usage*; Mintel Group Ltd, 2022. https://store.mintel.com/report/aircare-us-2022.

(23) Roberts, D. The Health Risks of Incense Use in the Home: An Underestimated Source of Indoor Air Pollution? *Community Practitioner: The Journal of the Community Practitioners' & Health Visitors' Association* **2016**, *89*, 36–41.

(24) Jones, R. P.; Jackson, N.; Orcés, D.; Huff, I. *The 2020 Census of American Religion*. Public Religion Research Institute, 2021. https://www.prri.org/research/2020-census-of-american-religion/.

(25) Mohamed, B.; Cox, K.; Diamant, J.; Gecewicz, C. *Faith Among Black Americans*. Pew Research Center, 2021; Chapter 4. https://www.pewresearch.org/religion/2021/02/16/faith-among-black-americans/.

(26) Cooperman, A.; Lopez, M., H.; Funk, C.; Martínez, J., H.; Ritchey, K. *The Shifting Religious Identity of Latinos in the United States*. Pew Research Center, 2014; Chapter 8. https://www.pewresearch.org/religion/2014/05/07/the-shifting-religious-identity-of-latinos-in-the-united-states/.

(27) Tonne, C. C.; Whyatt, R. M.; Camann, D. E.; Perera, F. P.; Kinney, P. L. Predictors of personal polycyclic aromatic hydrocarbon exposures among pregnant minority women in New York City. *Environmental Health Perspectives* **2004**, *112*, 754–759. https://doi.org/10.1289/ehp.5955.

(28) Wang, B.; Lee, S. C.; Ho, K. F. Chemical composition of fine particles from incense burning in a large environmental chamber. *Atmospheric Environment* **2006**, *40*, 7858–7868. https://doi.org/10.1016/j.atmosenv.2006.07.041.

(29) See, S. W.; Balasubramanian, R. Characterization of fine particle emissions from incense burning. *Building and Environment* **2011**, *46*, 1074–1080. https://doi.org/10.1016/j.buildenv.2010.11.006.

(30) Kuo, S.-C.; Tsai, Y. I.; Sopajaree, K. Emission identification and health risk potential of allergy-causing fragrant substances in $PM_{2.5}$ from incense Burning. *Building and Environment* **2015**, *87*, 23–33. https://doi.org/10.1016/j.buildenv.2015.01.012.

(31) Manoukian, A.; Buiron, D.; Temime-Roussel, B.; Wortham, H.; Quivet, E. Measurements of VOC/SVOC emission factors from burning incenses in an environmental test chamber: influence of temperature, relative humidity, and air exchange rate. *Environmental Science and Pollution Research* **2016**, *23*, 6300–6311. https://doi.org/10.1007/s11356-015-5819-2.

(32) Tsai, Y. I.; Wu, P.-L.; Hsu, Y.-T.; Yang, C.-R. Anhydrosugar and sugar alcohol organic markers associated with carboxylic acids in particulate matter from incense burning.

Atmospheric Environment **2010**, *44*, 3708–3718.
https://doi.org/10.1016/j.atmosenv.2010.06.030.

(33) Chuang, H.-C.; Jones, T.; Chen, Y.; Bell, J.; Wenger, J.; BéruBé, K. Characterisation of airborne particles and associated organic components produced from incense burning. *Analytical and Bioanalytical Chemistry* **2011**, *401*, 3095–3102. https://doi.org/10.1007/s00216-011-5209-7.

(34) Li, Y. J.; Yeung, J. W.; Leung, T. P.; Lau, A. P.; Chan, C. K. Characterization of Organic Particles from Incense Burning Using an Aerodyne High-Resolution Time-of-Flight Aerosol Mass Spectrometer. *Aerosol Science and Technology* **2012**, *46*, 654–665. https://doi.org/10.1080/02786826.2011.653017.

(35) Tran, T. C.; Marriott, P. J. Comprehensive two-dimensional gas chromatography – time-of-flight mass spectrometry and simultaneous electron capture detection/nitrogen phosphorous detection for incense analysis. *Atmospheric Environment* **2008**, *42*, 7360–7372. https://doi.org/10.1016/j.atmosenv.2008.06.028.

(36) Zhang, H.; Yee, L. D.; Lee, B. H.; Curtis, M. P.; Worton, D. R.; Isaacman-VanWertz, G.; Offenberg, J. H.; Lewandowski, M.; Kleindienst, T. E.; Beaver, M. R. Monoterpenes Are the Largest Source of Summertime Organic Aerosol in the Southeastern United States. *Proceedings of the National Academy of Sciences* **2018**, *115*, 2038–2043. https://doi.org/10.1073/pnas.1717513115.

(37) Jen, C. N.; Hatch, L. E.; Selimovic, V.; Yokelson, R. J.; Weber, R.; Fernandez, A. E.; Kreisberg, N. M.; Barsanti, K. C.; Goldstein, A. H. Speciated and total emission factors of particulate organics from burning western US wildland fuels and their dependence on combustion efficiency. *Atmospheric Chemistry and Physics* **2019**, *19*, 1013–1026. https://doi.org/10.5194/acp-19-1013-2019.

(38) Song, K.; Tang, R.; Li, A.; Wan, Z.; Zhang, Y.; Gong, Y.; Lv, D.; Lu, S.; Tan, Y.; Yan, S.; Yan, S.; Zhang, J.; Fan, B.; Chan, C. K.; Guo, S. Particulate organic emissions from incense-burning smoke: Chemical compositions and emission characteristics. *Science of The Total Environment* **2023**, *897*, 165319. https://doi.org/10.1016/j.scitotenv.2023.165319.

(39) Isaacman, G.; Kreisberg, N. M.; Yee, L. D.; Worton, D. R.; Chan, A. W. H.; Moss, J. A.; Hering, S. V.; Goldstein, A. H. Online derivatization for hourly measurements of gas- and particle-phase semi-volatile oxygenated organic compounds by thermal desorption aerosol gas chromatography (SV-TAG). *Atmospheric Measurement Techniques* **2014**, *7*, 4417–4429. https://doi.org/10.5194/amt-7-4417-2014.

(40) Abdullahi, K. L.; Delgado-Saborit, J. M.; Harrison, R. M. Emissions and indoor concentrations of particulate matter and its specific chemical components from cooking: A

679   review. *Atmospheric Environment* **2013**, *71*, 260–294.
680   https://doi.org/10.1016/j.atmosenv.2013.01.061.

681 (41) Pagels, J.; Wierzbicka, A.; Nilsson, E.; Isaxon, C.; Dahl, A.; Gudmundsson, A.; Swietlicki,
682   E.; Bohgard, M. Chemical composition and mass emission factors of candle smoke
683   particles. *Journal of Aerosol Science* **2009**, *40*, 193–208.
684   https://doi.org/10.1016/j.jaerosci.2008.10.005.

685 (42) DeCarlo, P. F.; Avery, A. M.; Waring, M. S. Thirdhand smoke uptake to aerosol particles in
686   the indoor environment. *Science Advances* **2018**, *4*, eaap8368.
687   https://doi.org/10.1126/sciadv.aap8368.

688 (43) Abbatt, J. P. D.; Wang, C. The atmospheric chemistry of indoor environments.
689   *Environmental Science: Processes & Impacts* **2020**, *22*, 25–48.
690   https://doi.org/10.1039/C9EM00386J.

691 (44) Weschler, C. J.; Nazaroff, W. W. Semivolatile organic compounds in indoor environments.
692   *Atmospheric Environment* **2008**, *42*, 9018–9040.
693   https://doi.org/10.1016/j.atmosenv.2008.09.052.

694 (45) Weschler, C. J.; Nazaroff, W. W. SVOC partitioning between the gas phase and settled dust
695   indoors. *Atmospheric Environment* **2010**, *44*, 3609–3620.
696   https://doi.org/10.1016/j.atmosenv.2010.06.029.

697 (46) Kristensen, K.; Lunderberg, D. M.; Liu, Y.; Misztal, P. K.; Tian, Y.; Arata, C.; Nazaroff, W.
698   W.; Goldstein, A. H. Gas–Particle Partitioning of Semivolatile Organic Compounds in a
699   Residence: Influence of Particles from Candles, Cooking, and Outdoors. *Environmental*
700   *Science & Technology* **2023**, *57*, 3260–3269. https://doi.org/10.1021/acs.est.2c07172.

701 (47) Lunderberg, D. M.; Kristensen, K.; Tian, Y.; Arata, C.; Misztal, P. K.; Liu, Y.; Kreisberg,
702   N.; Katz, E. F.; DeCarlo, P. F.; Patel, S.; Vance, M. E.; Nazaroff, W. W.; Goldstein, A. H.
703   Surface Emissions Modulate Indoor SVOC Concentrations through Volatility-Dependent
704   Partitioning. *Environmental Science & Technology* **2020**, *54*, 6751–6760.
705   https://doi.org/10.1021/acs.est.0c00966.

706 (48) Liu, C.; Morrison, G. C.; Zhang, Y. Role of aerosols in enhancing SVOC flux between air
707   and indoor surfaces and its influence on exposure. *Atmospheric Environment* **2012**, *55*, 347–
708   356. https://doi.org/10.1016/j.atmosenv.2012.03.030.

709 (49) Andersen, H. V.; Jørgensen, R. B.; Gunnarsen, L. Impact of smoking and candle burning on
710   air concentrations of PCB in a PCB contaminated indoor environment. *Atmospheric*
711   *Environment* **2023**, *309*, 119922. https://doi.org/10.1016/j.atmosenv.2023.119922.

712 (50) Zhao, Y.; Kreisberg, N. M.; Worton, D. R.; Teng, A. P.; Hering, S. V.; Goldstein, A. H.
713   Development of an in Situ Thermal Desorption Gas Chromatography Instrument for

Quantifying Atmospheric Semi-Volatile Organic Compounds. *Aerosol Science and Technology* **2013**, *47*, 258–266. https://doi.org/10.1080/02786826.2012.747673.

(51) Kristensen, K.; Lunderberg, D. M.; Liu, Y.; Misztal, P. K.; Tian, Y.; Arata, C.; Nazaroff, W. W.; Goldstein, A. H. Sources and dynamics of semivolatile organic compounds in a single-family residence in northern California. *Indoor Air* **2019**, *29*, 645–655. https://doi.org/10.1111/ina.12561.

(52) Liang, Y.; Jen, C. N.; Weber, R. J.; Misztal, P. K.; Goldstein, A. H. Chemical composition of PM$_{2.5}$ in October 2017 Northern California wildfire plumes. *Atmospheric Chemistry and Physics* **2021**, *21*, 5719–5737. https://doi.org/10.5194/acp-21-5719-2021.

(53) Franklin, E. B.; Yee, L. D.; Aumont, B.; Weber, R. J.; Grigas, P.; Goldstein, A. H. Ch3MS-RF: a random forest model for chemical characterization and improved quantification of unidentified atmospheric organics detected by chromatography–mass spectrometry techniques. *Atmospheric Measurement Techniques* **2022**, *15*, 3779–3803. https://doi.org/10.5194/amt-15-3779-2022.

(54) Mazzoleni, L. R.; Zielinska, B.; Moosmüller, H. Emissions of Levoglucosan, Methoxy Phenols, and Organic Acids from Prescribed Burns, Laboratory Combustion of Wildland Fuels, and Residential Wood Combustion. *Environmental Science & Technology* **2007**, *41*, 2115–2122. https://doi.org/10.1021/es061702c.

(55) Oros, D. R.; Simoneit, B. R. T. Identification and emission factors of molecular tracers in organic aerosols from biomass burning part 1. Temperate climate conifers. *Applied Geochemistry* **2001**, *16*, 1513–1544. https://doi.org/10.1016/S0883-2927(01)00021-X.

(56) Hays, M. D.; Geron, C. D.; Linna, K. J.; Smith, N. D.; Schauer, J. J. Speciation of Gas-Phase and Fine Particle Emissions from Burning of Foliar Fuels. *Environmental Science & Technology* **2002**, *36*, 2281–2295. https://doi.org/10.1021/es0111683.

(57) Liang, Y.; Stamatis, C.; Fortner, E. C.; Wernis, R. A.; Van Rooy, P.; Majluf, F.; Yacovitch, T. I.; Daube, C.; Herndon, S. C.; Kreisberg, N. M.; Barsanti, K. C.; Goldstein, A. H. Emissions of organic compounds from western US Wildfires and their near-fire transformations. *Atmospheric Chemistry and Physics* **2022**, *22*, 9877–9893. https://doi.org/10.5194/acp-22-9877-2022.

(58) Sigsgaard, T.; Forsberg, B.; Annesi-Maesano, I.; Blomberg, A.; Bølling, A.; Boman, C.; Bønløkke, J.; Brauer, M.; Bruce, N.; Héroux, M.-E. Health impacts of anthropogenic biomass burning in the developed world. *European Respiratory Journal* **2015**, *46*, 1577–1588. https://doi.org/10.1183/13993003.01865-2014.

(59) Liu, L.; Liu, Y.; Lin, J.; Tang, N.; Hayakawa, K.; Maeda, T. Development of analytical methods for polycyclic aromatic hydrocarbons (PAHs) in airborne particulates: A review.

Journal of Environmental Sciences **2007**, *19*, 1–11. https://doi.org/10.1016/S1001-0742(07)60001-1.

(60) Lung, S.-C. C.; Hu, S.-C. Generation rates and emission factors of particulate matter and particle-bound polycyclic aromatic hydrocarbons of incense sticks. *Chemosphere* **2003**, *50*, 673–679. https://doi.org/10.1016/S0045-6535(02)00613-6.

(61) Yeoman, A. M.; Shaw, M.; Ward, M.; Ives, L.; Andrews, S. J.; Lewis, A. C. Gas Phase Emissions of Volatile Organic Compounds Arising from the Application of Sunscreens. *International Journal of Environmental Research and Public Health* **2023**, *20*, 5944. https://doi.org/10.3390/ijerph20115944.

(62) Kim, K.; Shin, H.-M.; Wong, L.; Young, T. M.; Bennett, D. H. Temporal variability of indoor dust concentrations of semivolatile organic compounds. *Indoor Air* **2021**, *31*, 693–701. https://doi.org/10.1111/ina.12759.

(63) Liu, Z.; Little, J. C. Semivolatile organic compounds (SVOCs): phthalates and flame retardants. In *Toxicity of Building Materials*; Elsevier, 2012; pp 122–137. https://doi.org/10.1533/9780857096357.122.

(64) Lunderberg, D. M.; Kristensen, K.; Liu, Y.; Misztal, P. K.; Tian, Y.; Arata, C.; Wernis, R.; Kreisberg, N.; Nazaroff, W. W.; Goldstein, A. H. Characterizing Airborne Phthalate Concentrations and Dynamics in a Normally Occupied Residence. *Environmental Science & Technology* **2019**, *53*, 7337–7346. https://doi.org/10.1021/acs.est.9b02123.

(65) Risk Science Center, Department of Environmental Health, University of Cincinnati. *Toxicity Review for Di-2-Ethylhexyl Terephthalate (DEHT)*. Report No. CPSC-D-17-0001; University of Cincinnati, 2018. https://www.CPSC.gov.

(66) Shields, H. C.; Fleischer, D. M.; Weschler, C. J. Comparisons among VOCs Measured in Three Types of U.S. Commercial Buildings with Different Occupant Densities. *Indoor Air* **1996**, *6*, 2–17. https://doi.org/10.1111/j.1600-0668.1996.t01-3-00002.x.

(67) Fortenberry, C.; Walker, M.; Dang, A.; Loka, A.; Date, G.; Cysneiros de Carvalho, K.; Morrison, G.; Williams, B. Analysis of indoor particles and gases and their evolution with natural ventilation. *Indoor Air* **2019**, *29*, 761–779. https://doi.org/10.1111/ina.12584.

(68) Yadav, V. K.; Malik, P.; Tirth, V.; Khan, S. H.; Yadav, K. K.; Islam, S.; Choudhary, N.; Inwati, G. K.; Arabi, A.; Kim, D.-H.; Jeon, B.-H. Health and Environmental Risks of Incense Smoke: Mechanistic Insights and Cumulative Evidence. *Journal of Inflammation Research* **2022**, *15*, 2665–2693. https://doi.org/10.2147/JIR.S347489.

(69) Xu, Y.; Little, J. C. Predicting Emissions of SVOCs from Polymeric Materials and Their Interaction with Airborne Particles. *Environmental Science & Technology* **2006**, *40*, 456–461. https://doi.org/10.1021/es051517j.

784 (70) Benning, J. L.; Liu, Z.; Tiwari, A.; Little, J. C.; Marr, L. C. Characterizing Gas-Particle
785   Interactions of Phthalate Plasticizer Emitted from Vinyl Flooring. *Environmental Science &*
786   *Technology* **2013**, *47*, 2696–2703. https://doi.org/10.1021/es304725b.

787 (71) Salthammer, T.; Zhang, Y.; Mo, J.; Koch, H. M.; Weschler, C. J. Assessing Human Exposure
788   to Organic Pollutants in the Indoor Environment. *Angewandte Chemie International Edition*
789   **2018**, *57*, 12228–12263. https://doi.org/10.1002/anie.201711023.

790 (72) Rudel, R. A.; Perovich, L. J. Endocrine disrupting chemicals in indoor and outdoor air.
791   *Atmospheric Environment* **2009**, *43*, 170–181.
792   https://doi.org/10.1016/j.atmosenv.2008.09.025.

793 (73) Aiken, A. C.; DeCarlo, P. F.; Kroll, J. H.; Worsnop, D. R.; Huffman, J. A.; Docherty, K. S.;
794   Ulbrich, I. M.; Mohr, C.; Kimmel, J. R.; Sueper, D.; Sun, Y.; Zhang, Q.; Trimborn, A.;
795   Northway, M.; Ziemann, P. J.; Canagaratna, M. R.; Onasch, T. B.; Alfarra, M. R.; Prevot, A.
796   S. H.; Dommen, J.; Duplissy, J.; Metzger, A.; Baltensperger, U.; Jimenez, J. L. O/C and
797   OM/OC Ratios of Primary, Secondary, and Ambient Organic Aerosols with High-Resolution
798   Time-of-Flight Aerosol Mass Spectrometry. *Environmental Science & Technology* **2008**, *42*,
799   4478–4485. https://doi.org/10.1021/es703009q.

800 (74) Canagaratna, M. R.; Jimenez, J. L.; Kroll, J. H.; Chen, Q.; Kessler, S. H.; Massoli, P.;
801   Hildebrandt Ruiz, L.; Fortner, E.; Williams, L. R.; Wilson, K. R.; Surratt, J. D.; Donahue, N.
802   M.; Jayne, J. T.; Worsnop, D. R. Elemental ratio measurements of organic compounds using
803   aerosol mass spectrometry: characterization, improved calibration, and implications.
804   *Atmospheric Chemistry and Physics* **2015**, *15*, 253–272. https://doi.org/10.5194/acp-15-253-
805   2015.

806 (75) Nazaroff, W. W. Inhalation intake fraction of pollutants from episodic indoor emissions.
807   *Building and Environment* **2008**, *43*, 269–277.
808   https://doi.org/10.1016/j.buildenv.2006.03.021.

809 (76) Chan, W. R.; Logue, J. M.; Wu, X.; Klepeis, N. E.; Fisk, W. J.; Noris, F.; Singer, B. C.
810   Quantifying fine particle emission events from time-resolved measurements: Method
811   description and application to 18 California low-income apartments. *Indoor Air* **2018**, *28*,
812   89–101. https://doi.org/10.1111/ina.12425.

813 (77) Mage, D. T.; Ott, W. R. Accounting for Nonuniform Mixing and Human Exposure in Indoor
814   Environments. In Tichenor, B. A. (Ed.), *Characterizing Sources of Indoor Air Pollution and*
815   *Related Sink Effects, ASTM STP 1287,* American Society for Testing and Materials **1996**, No.
816   1287, pp. 263–278.

817 (78) Yang, C.-R.; Lin, T.-C.; Chang, F.-H. Correlation between Calcium Carbonate Content and
818   Emission Characteristics of Incense. *Journal of the Air & Waste Management Association*
819   **2006**, *56*, 1726–1732. https://doi.org/10.1080/10473289.2006.10464577.

1   *Supporting Information for*

2   **Characterizing PM$_{2.5}$ Emissions and Temporal Evolution of Organic**

3   **Composition from Incense Burning in a California Residence**

4   Jennifer Ofodile*, Michael R. Alves, Yutong Liang, Emily B. Franklin, David M. Lunderberg,

5   Cesunica E. Ivey, Brett C. Singer, William W Nazaroff, and Allen H. Goldstein

6   *Corresponding Author: jofodile@berkeley.edu

7 **Supporting Information:**

8 Includes 17 pages, 6 experimental descriptions, 3 figures, and 11 tables.

9 Experimental:

16 Tables:

34 Figures:

Field Campaign and Study Site

Incense burning measurements analyzed in this study were conducted in a normally occupied single-family residence (designated H3 as the third installment in a series of indoor observational campaigns[1–3]) located in a residential area of Oakland, California. The H3 residence was the study site of a much larger effort that entailed a continuous observational indoor monitoring campaign. The decision to investigate incense burning as a source of fine particle-phase organics in this residence was intended to contribute new knowledge about the influence of an important indoor emission source on indoor air chemistry. This specific site also served as a matter of convenience for the incense experiments explored in the current study. Although no individual house can be fully representative of all residential conditions, the H3 residence is a common example of older construction (50-100 yr. old) single-family homes in urban core areas of the west coast of the US.

The H3 observational campaign spanned 10 weeks from early October to early December 2021. H3 is a wood-framed detached home initially constructed in the 1910s as a 1200 square foot (sf) dwelling consisting of two bedrooms, one bathroom, a kitchen, dining room, and living room. These rooms are situated over an enclosed, dry, and well-ventilated standing height basement that functions as both a garage and a storage area. A 600-sf two-story addition was constructed at the back of the house in 1960 and adds a bedroom, bathroom, and office upstairs with an open bonus room downstairs at ground level. The kitchen is outfitted with hardwood flooring, located at the back of the original structure, with open doorways to the dining room and one bedroom in the main original structure as well as to the upstairs hallway in the addition. At the time of the study, the house had a central forced air, natural gas furnace with supply registers located in each room of the original structure and on each floor of the addition with a single return register in the dining room. This system was equipped with a MERV 13 air filter and controlled with a programmable thermostat. The occupants of H3 comprised one adult male, one adult female, and one cat. They lived in H3 residence as usual during the monitoring campaign. During the incense experiments, H3 occupants were away from the house for several days. By normal practice of the residents, the home was generally well-ventilated throughout the campaign by opening of multiple windows during each day. However, during the incense burning experiments, all exterior doors and windows were kept closed.

Detailed Incense Experiments and PM$_{2.5}$ Sample Collection

Incense smoke was sampled in H3 kitchen through a custom designed aerosol sampler (DEFCON, UCB Goldstein Lab) with prior applications in biomass burning campaigns.[4,5] DEFCON's inlet housed a 2.5 µm sharp cut cyclone (BGI by Mesa Laboratories, SCC2.654) with an airstream flow at 10 L min^{-1} and downstream collection of airborne particle-phase (PM$_{2.5}$) aerosol on 47 mm quartz fiber filters (Pallflex, Tissuequartz). Flow rates were measured and monitored with a data logger (DATAQ Instruments, DI-2108) to verify constant flow at the target rate. Prior to sample collection, quartz fiber filters were thermally prepared by baking at 550 °C for 12 h before being individually stored in pre-baked aluminum foil, sealed in mylar bags, and packed in secondary plastic Ziploc bags.

83 At H3, two different types of incense sticks were used in burning experiments. Lavender and
84 Douglas fir incense were purchased from a local supermarket, having been produced in India and
85 California, respectively. The selection of the incense scents burned in the study residence depended
86 on the preferences of H3 occupants. While the choice of incense scents by end users may be very
87 subjective, lavender and wood-based scents like Douglas fir are among the most popular and
88 relatively well-represented incense scents on the market.

89 Before incense experiments, a background sample of the indoor air at H3 was collected in the
90 kitchen over a 22-h period. H3 occupants reported that they had never burned incense during their
91 20-yr occupancy of the house. As a result, the background sample is assumed to be representative
92 of the H3 indoor environment, unperturbed by incense-related combustion products. Occupants
93 departed from the H3 residence the night prior to indoor background sampling. The gas-fired
94 furnace was off and all windows and doors to the outdoors were closed throughout the vacant
95 period (except for brief door opening for the ingress and egress of researchers).

96 Five incense experiments were carried out in all, once for lavender incense and four times for
97 Douglas fir incense, with burns occurring twice a day around noon and 5:30 pm. Incense
98 experiments were completed using two incense sticks for each "burn". Both sticks were ignited
99 simultaneously in the kitchen and allowed to burn to completion over a ~60-min duration
100 designated as the burning period (see Figure S1). Following the burning period, the incense source
101 (uncoated stick remnants and tray holder) was removed from the kitchen and the H3 residence.
102 Indoor filter sampling started on average 8 min prior to incense ignition. Samples were collected
103 over 6-h periods on average, with one sample (DougFir-2) running through the night. Incense
104 emissions during the burning period of the fourth experiment for Douglas fir incense (DougFir-4)
105 were disturbed as one of the two sticks did not burn to completion once lit and needed to be
106 reignited several times. We observed lower $PM_{2.5}$ organics attributed to incense for this DougFir-
107 4 experiment compared to others, which was likely a result of this incomplete combustion behavior
108 after the initial ignition.

109 All H3 indoor samples were collected under closed home conditions, except for brief entry by a
110 researcher to set up and remove sampling equipment. Three outdoor air samples, coinciding with
111 indoor sampling periods, were collected using a second DEFCON sampler placed on the wooden
112 deck in the small back yard with vegetation outside the H3 residence. Field blanks were collected
113 before each indoor and outdoor sample to estimate contributions from sampling components and
114 the kitchen indoor air. After sample collection, all filters were returned to their initial storage form
115 and frozen (-20 ℃) prior to instrument analysis.
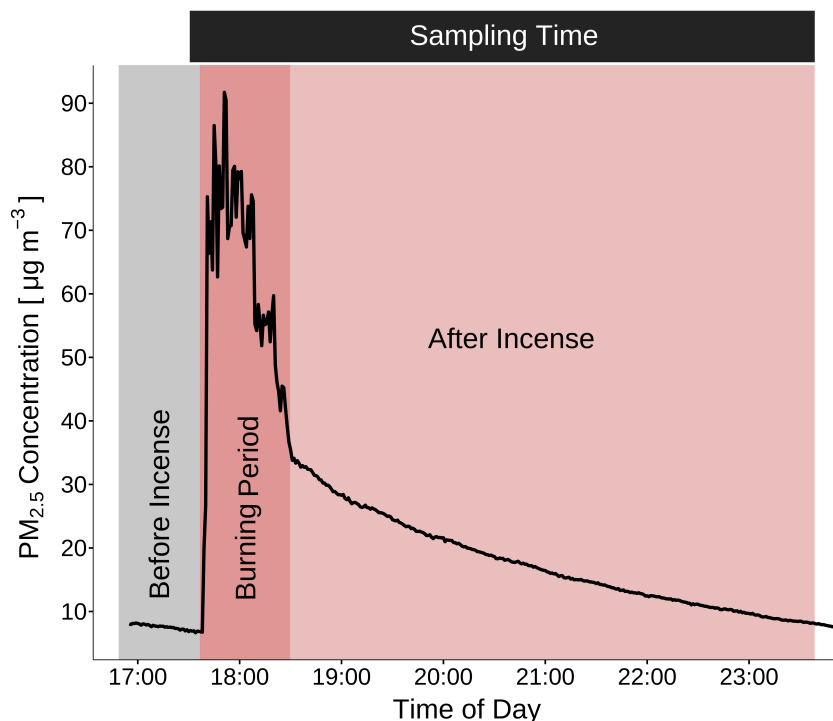
Figure S1. Time-resolved PM$_{2.5}$ concentrations by Particles Plus during a Douglas fir incense burn, separated by three experiment periods. The burning period for incense sticks is ~60 min followed by the removal of the incense source from H3 at its conclusion. The sampling period begins before incense combustion and is 6 h on average.

Detailed PM$_{2.5}$ Filter Analysis and Quantification: GC×GC

PM$_{2.5}$ filters collected in H3 were analyzed by offline thermal desorption two-dimensional gas chromatography with online derivatization coupled with electron ionization high resolution time-of-flight mass spectrometry (TD-GC×GC-EI-HR-ToF-MS). A complete methodological description of this instrument has been published[6] and instrument specifications are summarized in Table S1. Filter punches (0.07-0.82 cm^2) from all H3 filters were impregnated with isotopically labeled internal standards (Table S2) prior to analysis to correct for matrix effects and instrument performance. During thermal desorption of filter punches at 320 °C, a derivatization agent, N-methyl-N-(trimethylsilyl)trifluoroacetamide (MSTFA), was introduced to the helium gas flow. Online derivatization replaces the active hydrogen in −OH, −SH, and −NH$_2$ groups with a trimethylsilyl group, −Si(CH$_3$)$_3$, which enables easier elution and enhanced recovery of polar organic compounds. Thermally desorbed compounds were trapped on a 30 °C cooled inlet system with a quartz wool glass liner before injection into the GC system. Compounds were separated by volatility in the first column and then by polarity in the second column, with transfer between the two columns being cryogenically modulated (2.3 s). Separated compounds were then ionized by 70 eV electron impact before detection by HR-ToF-MS with a resolving power of 4000. The volatility range of this analysis spans between ~C$_{13}$ and ~C$_{36}$ n-alkane volatility equivalents, accounting largely for semivolatile organic compounds (SVOCs), and some intermediate volatility organic compounds (IVOCs) and low volatility organic compounds (LVOCs).

For compound quantification, external standard mixtures of 110 compounds were prepared on quartz fiber filters and analyzed identically to sample filters. Both standard compounds and sample analytes were normalized (i.e., divided) by the average of the three nearest internal standards. Each internal standard compound is initially self-normalized by its respective mean across all GC×GC chromatograms during the analysis period. This normalization process ensures that any variations in instrument response of the internal standards are accounted for and prevents artificial inflation or deflation of quantified compounds.[7] The authentic standards used in this work were selected for corresponding and relating to analytes observed in incense smoke and indoor environments. As such, 82 standard compounds were biomass-burning (BB) related (e.g., alkanes, acids, sugars, etc.) while the remaining 28 were indoor-specific (e.g., phthalates, esters, pesticides, etc.). The full list of external standard components is given in Tables S3 and S4. Six-point calibration curves ($R^2 >$ 0.90) for all external standards were generated and used to quantify compounds in H3 samples. Sample analytes matching an external standard were directly quantified while sample compounds not present in the standard mix were quantified by a proxy standard assignment.[4,8] Sample compounds in the same chemical family as an existing standard were quantified using the closest external standard in that family. For unidentifiable and unknown compounds, the nearest external standard in 2D space was used for quantification. Mass loadings of quantified compounds were first blank subtracted when applicable before converting observed signals to mass concentrations using sampling duration and flow rate data. The quantification method described has approximate uncertainties of ±10% for standard matched compounds, ±30% for classified compounds using the nearest standard in the same family, and a systematic uncertainty of 200% for unknown compounds.[4]

Table S1. Instrument Specifications and Materials.

	TD-GC×GC-EI-HR-ToF-MS
Carrier gas	Helium: 2 ml min^{-1}
Thermal desorption unit	Gerstel: TDS-3 and TDSA2
Thermal desorption temperature	320 °C
Cooled inlet system material	Gerstel: CIS4 (quartz wool)
Cooled inlet system temperature	Trap: 30 °C Release: 320 °C
Oven	Agilent: 7890A
Column 1 material	Restek, Rxi-5Sil MS: 60 m × 0.25 mm × 0.25 μm
Column 1 temperature	3.5 °C min^{-1} from 40 to 320 °C Hold: 5 min at 320 °C
Column 2 material	Restek, Rtx-200 MS: 1 m × 0.25 mm × 0.25 μm
Column 2 temperature	15 °C higher than column 1
Thermal dual-stage modulator	ZOEX
Guard column	Restek, Siltek: 1.5m × 0.25mm × 250 μm
Modulation period	2.3 s
Ionization	70 eV
Ionization chamber temperature	270 °C
Mass spectrometer	Tofwerk: HR-ToF-MS (m/Δm = 4000)

163 **Table S2. Deuterated Internal Standard Compounds Applied to Each Filter Sample.**

Internal Standard Compounds	
2^{13}C-pentaerythritol	d46-C22 alkane
C12 diacid	d50-C24 alkane
C6 diacid	d51-C26 acid
d10-phenanthrene	d5-3-hydroxyglutaric acid
d10-pyrene	d54-C26 alkane
d12-chrysene	d5-4-hydroxybenzaldehyde
d12-perylene	d58-C28 alkane
d21-decanol	d5-benzoic acid
d25-dodecanol	d5-C10 acid
d31-pentadecanol	d5-cholestane
d34-C16 alkane	d62-C30 alkane
d35-C18 acid	d66-C32 alkane
d37-octadecanol	d6-syringic Acid
d38-C18 alkane	d70-C34 alkane
d41-eicosanol	d74-C36 alkane
d42-C20 alkane	d7-cholesterol
d43-C22 acid	d8-anthraquinone
d4-4-methoxy-benzaldehyde	d8-methylcatechol

164 **Table S3. Indoor-Specific Authentic External Standards.**

External Standard Compounds (Indoor)					
Compound Name	RT2	RI[a]	Compound Name	RT2	RI[a]
1-Nonanol	0.46	1262	Diethyl phthalate	1.32	1587
2,4-Dihydroxybenzophenone	1.00	2146	Dimethyl phthalate	1.46	1449
2,5-Di-tert-butyl-1,4-benzoquinone	1.05	1474	Ethylparaben	0.95	1565
2-Phenoxyethanol	0.67	1357	Galaxolide	0.74	1849
4-Nonlyphenol	0.58	1921	Homosalate	0.85	2019
Anethole	0.79	1277	Isopropyl myristate	0.67	1822
Benzophenone	1.09	1635	Methyl salicylate	0.91	1394
Benzyl butyl phthalate	1.15	2345	Methylparaben	0.98	1494
Bis(2-ethylhexyl) phthalate	0.96	2531	Propylparaben	0.93	1662
Butylparaben	0.90	1766	Tonalid	1.03	1858
Carvacrol	0.59	1320	Trimethyl pentanediol diisobutyrate	1.04	1589
D6 siloxane	0.49	1290	Tripropylene glycol monomethyl ether	0.58	1426
DEET (Diethyltoluamide)	1.62	1576	Tris(2-chloroethyl) phosphate	1.79	1757
Dibutyl phthalate	1.13	1954	α-Terpineol	0.52	1312

[a]RI is based on linear *n*-alkanes

165   **Table S4. Biomass-Burning Related Authentic External Standards.**

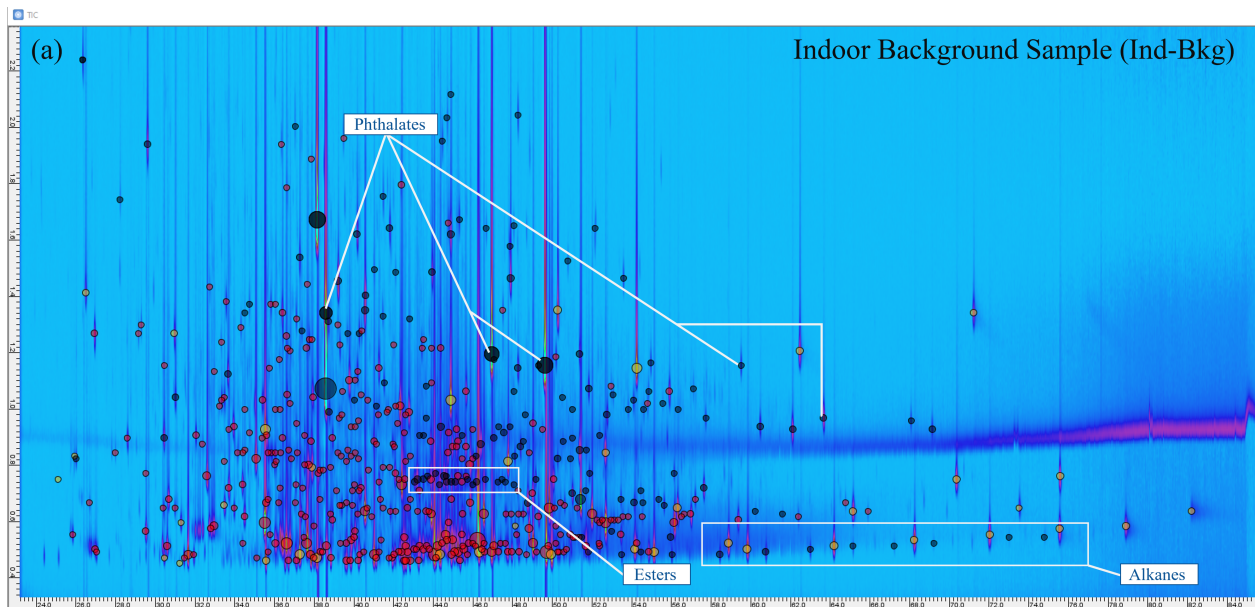| External Standard Compounds (BB)					
Compound Name	RT2	RI[a]	Compound Name	RT2	RI[a]
1,2-Benzanthracene	1.17	2474	C28 alkane	0.53	2800
2,4-Dinitrophenol	2.24	1753	C28 carboxylic acid	0.67	3231
3,5-Dimethoxyphenol	0.80	1503	C29 alkane	0.54	2900
4-Hydroxybenzoic acid	0.83	1625	C30 alkane	0.54	3000
4-Methylcatechol	0.59	1383	C31 alkane	0.55	3100
4-Nitrocatechol	1.46	1742	C32 alkane	0.56	3200
5-(Hydroxymethyl) furfural	1.25	1301	C33 alkane	0.57	3300
5-Nitrovanillin	1.92	1834	C34 alkane	0.59	3400
Abietic acid	0.75	2425	C35 alkane	0.62	3500
Acenaphthylene	0.95	1459	C36 alkane	0.65	3600
Anthracene	1.03	1805	C9 carboxylic acid	0.64	1354
Benzo(a)pyrene	1.34	2886	Cholesterol	0.79	3153
Benzo(b)fluoranthene	1.33	2794	Chrysene	1.19	2484
Benzo(g,h,i)perylene	1.48	3279	D-(+)-mannose	0.56	1795
Benzo(k)fluoranthene	1.33	2802	Dibenz(a,h)anthracene	1.39	3217
C10 carboxylic acid	0.64	1457	D-pinitol	0.55	1825
C11 carboxylic acid	0.63	1554	Ergosterol	0.77	3236
C12 carboxylic acid	0.64	1651	Fluoranthene	1.13	2078
C13 carboxylic acid	0.63	1748	Fluorene	0.88	1593
C14 carboxylic acid	0.63	1847	Hexadecane, 2,6,10,14-tetramethyl-	0.49	1807
C15 carboxylic acid	0.63	1944	Hydroquinone	0.67	1397
C16 alkane	0.45	1600	Indeno(1,2,3-cd)pyrene	1.46	3207
C16 carboxylic acid	0.63	2043	Isopimaric acid	0.78	2343
C17 alkane	0.46	1700	Levoglucosan	0.78	1698
C17 carboxylic acid	0.62	2141	Maltol	1.02	1270
C18 alkane	0.46	1800	p-Anisic acid (4-methoxybenzoic acid)	0.88	1521
C18 carboxylic acid	0.62	2240	Pentadecane, 2,6,10,14-tetramethyl-	0.48	1704
C19 alkane	0.47	1900	Phenanthrene	1.03	1795
C20 alkane	0.47	2000	Pyrene	1.16	2137
C20 carboxylic acid	0.62	2439	Pyrocatechol (Catechol)	0.62	1303
C21 alkane	0.47	2100	Resorcinol	0.66	1376
C22 alkane	0.48	2200	Retene	0.97	2227
C22 carboxylic acid	0.64	2637	Sinapinalehyde	1.43	2000
C23 alkane	0.49	2300	Stigmasterol	0.80	3283
C23 carboxylic acid	0.64	2735	Syringaldehyde	1.25	1698
C24 alkane	0.50	2400	Syringic acid	0.81	1892
C24 carboxylic acid	0.64	2833	Syringol (2,6-Dimethoxyphenol)	0.75	1395
C25 alkane	0.50	2500	Vanillic acid	0.80	1760
C26 alkane	0.51	2600	Vanillin	1.25	1536
C26 carboxylic acid	0.65	3031	α-Amyrin	0.92	3417
C27 alkane	0.52	2700	β-Sitosterol	0.77	3345

[a]RI is based on linear n-alkanes

Compositional Analysis of Incense PM$_{2.5}$ Samples

GC×GC chromatograms were analyzed with GC informatics software (GC Image, LLC). Initial identification and classification of sample compounds into chemical families was accomplished through direct matches with authentic standards, as determined by matching mass spectra and retention times. Using the National Institute of Standards and Technology (NIST) Mass Spectral Search software, the remainder of unmatched compounds were searched against the NIST-20 mass spectral database and Goldstein Library of Biogenic and Environmental Spectra (UCB-GLOBES). UCB-GLOBES was created at UC Berkeley with MS library entries from previous studies using GC×GC.[4,8] Compound matching (match factor > 700) relies on the first-dimension volatility linear retention index (RI) that tracks the elution order from the first GC column. For compounds analyzed using the same instrument, the RI is expected to be analogous and factored into the analysis. Subsequent classification of compounds not readily identified by matching with external standards and MS libraries was achieved with RI and second dimension retention times (RT2) comparisons as well as examination of EI mass spectra for specific molecular ions that are representative of certain functional groups (e.g., m/z = 204 and m/z = 217 for derivatized sugars). Compounds that could not be identified or classified using these methods are reported as unknown.

GC×GC Derivatization Classification

External standard compounds such as alkanes, phthalates, PAHs, and esters without active hydrogens (e.g., −OH) were used to determine if a compound was derivatized in a sample. The criteria for this process used the intensity of the m/z = 73 ion, which is indicative of a derivatized compound as a result of $[Si(CH_3)_3]^{\bullet+}$, relative to (i.e., divided by and as a percentage of) the total intensity value of the EI multi-spectrum for each compound. For the standard compounds used, the threshold was a less than 5% contribution of the m/z = 73 ion intensity relative to the total intensity of the multi-spectrum. As a result, compounds within a sample that exhibited m/z = 73 ion intensities less than 5% were categorized as underivatized. Figure S2 shows the distribution of derivatized and underivatized compounds in the indoor background sample and burn samples of Douglas fir and lavender incense. On average, derivatized compounds accounted for 86% of all compounds detected and separated across all H3 samples. Black points highlighted in Figure S2 are underivatized compounds. Samples collected during incense burns had less than 12% of incense-attributed compounds underivatized while the indoor background sample had 30% underivatized compounds. Analysis with GC×GC coupled with online derivatization captures and retains polar and oxygenated compounds in incense smoke.

(a) Indoor Background Sample (Ind-Bkg)

Phthalates

Esters

Alkanes

198

(b) Incense sample (DougFir-1)

Phthalates

Dehydroabietic Acid

Levoglucosan

Esters

Alkanes

199

200
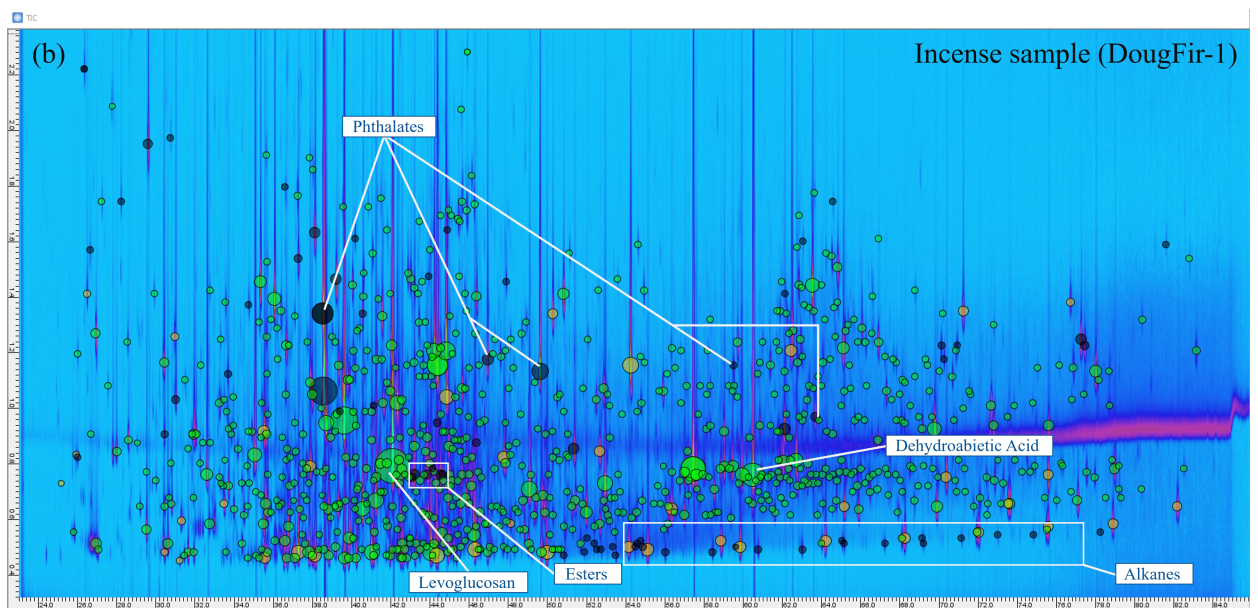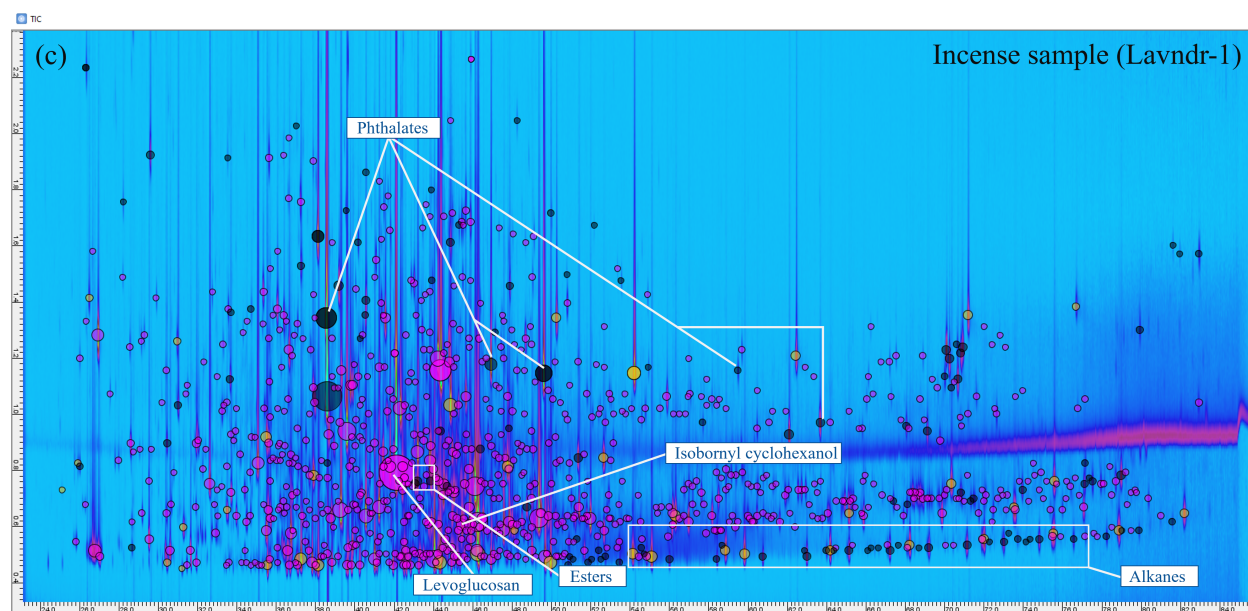
Figure S2. Incidence of derivatized compounds in (a) the indoor background sample and (b, c) in samples collected during Douglas fir and lavender incense burns, respectively. Red, green, and purple points in (a, b, c) represent derivatized sample compounds, black points represent underivatized sample compounds, and yellow points represent internal standard compounds.

Table S5. Speciated OA Mass Concentrations (µg m^{-3}) for Positively Identified Compounds Related to Biomass Burning and Possessing Hazard Codes.[9]

	Lavndr-1	DougFir-1	DougFir-2	DougFir-3	DougFir-4
Levoglucosan	1.31	0.91	1.05	1.20	0.43
Dehydroabietic acid	< 0.01	0.73	0.25	0.49	0.22
Tetracosanoic acid	0.08	0.13	0.08	0.10	0.06
Hexacosanoic acid	0.04	0.13	0.12	0.12	0.04
Pyrogallol	0.02	0.01	< 0.01	0.01	< 0.01
Galactosan	< 0.01	0.01	0.01	0.01	< 0.01
Vanillic acid	0.01	< 0.01	< 0.01	< 0.01	< 0.01
D-pinitol	0.02	< 0.01	< 0.01	–	–
4-Hydroxybenzoic acid	< 0.01	< 0.01	< 0.01	< 0.01	< 0.01
Catechol	0.02	–	–	0.01	–
Eicosanoic acid	0.06	0.05	0.04	0.04	0.03
Hexanedioic acid	0.05	0.07	0.01	0.02	0.02

Table S6. Speciated GC×GC OA Mass Concentrations (μg m⁻³) of Each Chemical Family for Total Incense-Attributed Mass Concentration from Each Incense Burn Sample.

	Lavndr-1	DougFir-1	DougFir-2	DougFir-3	DougFir-4
Acids	0.30	0.40	0.31	0.32	0.16
Alcohols	0.03	0.03	0.02	0.02	0.01
Alkanes	0.05	0.01	0.01	0.06	0.08
Aromatics	0.09	0.11	0.09	0.07	0.04
Cyclics/Oxy	0.56	0.56	0.40	0.31	0.14
Methoxyphenols	0.05	0.37	0.15	0.24	0.13
Other Oxy	0.11	0.30	0.11	0.23	0.08
Other Terpenoids	0.19	–	–	–	–
Resins/Diterpenoids	< 0.01	2.18	0.91	1.72	0.79
Sterols/Triterpenoids	0.07	0.26	0.15	0.20	0.08
Sugars	2.80	2.22	1.69	2.43	0.89
Not Identifiable	0.38	0.20	0.11	0.19	0.13
Unclassified	1.07	1.27	0.83	1.06	0.73

Table S7. Speciated GC×GC OA Mass Concentrations (μg m⁻³) of Each Chemical Family for Total Indoor Background Mass Concentration from Each Incense Burn Sample.

	Ind-Bkg	Lavndr-1	DougFir-1	DougFir-2	DougFir-3	DougFir-4
Acids	0.04	0.28	0.26	0.16	0.23	0.18
Alcohols	0.16	0.58	0.55	0.18	0.35	0.57
Alkanes	0.01	0.13	0.03	0.03	0.17	0.24
Aromatics	0.02	0.08	0.10	0.04	0.07	0.09
Cyclics/Oxy	0.01	0.01	0.01	0.01	0.01	0.01
Esters	0.07	0.15	0.16	0.08	0.15	0.21
Flame Retardants	0.03	0.10	0.02	0.06	0.04	0.08
Other Non-Cyclic Aliphatics/Oxy	0.01	0.01	0.01	0.01	< 0.01	0.01
Other Oxy	< 0.01	0.01	< 0.01	< 0.01	< 0.01	< 0.01
Pesticides	0.15	0.10	0.06	0.07	0.08	0.09
Plasticizers, Non-Phthalates	0.12	0.55	0.33	0.17	0.68	0.68
Plasticizers, Phthalates	0.14	0.28	0.21	0.14	0.18	0.25
Siloxanes	0.04	0.07	0.13	0.03	0.06	0.07
Surfactants	0.36	0.33	0.37	0.28	0.25	0.34
Not Identifiable	0.12	0.47	0.51	0.17	0.23	0.51
Unclassified	0.07	0.20	0.14	0.08	0.13	0.17

Table S8. Mean and Median Enhancement Ratios of Indoor Background Compounds
**Detected in Incense Samples.**[a]

Compound Identification	Chemical Family	RT2	RI[b]	Median	Mean
Azelaic acid, 2TMS[c]	Acids	0.86	1793	24.2	26.2
C10 carboxylic acid	Acids	0.64	1456	7.7	7.6
C12 carboxylic acid	Acids	0.63	1650	8.0	8.1
C13 carboxylic acid	Acids	0.63	1748	8.3	8.8
C20 carboxylic acid	Acids	0.62	2438	14.5	16.0
Hexanedioic acid, 2TMS	Acids	0.90	1503	8.6	11.9
1-Dodecanol, TMS	Alcohols	0.48	1567	4.6	4.0
1-Tetradecanol, TMS	Alcohols	0.48	1763	2.8	2.7
1-Tridecanol, TMS	Alcohols	0.48	1665	4.9	4.8
2-Tetradecanol, TMS	Alcohols	0.47	1688	4.9	4.9
C21 alkane	Alkanes	0.48	2100	4.9	4.6
C22 alkane	Alkanes	0.48	2200	4.7	5.8
C26 alkane	Alkanes	0.51	2600	40.3	36.4
C27 alkane	Alkanes	0.51	2700	46.5	42.8
C28 alkane	Alkanes	0.52	2800	51.5	41.5
C30 alkane	Alkanes	0.54	3000	16.2	12.9
C31 alkane	Alkanes	0.54	3100	10.1	8.1
2,6-Dimethoxyhydroquinone, 2O-TMS	Aromatics	0.73	1672	8.2	9.8
Homosalate, TMS	Aromatics	0.85	2019	5.3	5.6
Isophthalic acid, TMS	Aromatics	0.88	1756	7.2	6.7
Versalide	Aromatics	0.74	1850	4.3	5.1
γ-Dodecalactone	Cyclics/Oxy	1.75	1678	3.9	3.8
γ-Palmitolactone	Cyclics/Oxy	1.46	2103	2.6	2.7
Diisopropyl adipate	Esters	1.12	1448	2.8	2.8
Isopropyl myristate	Esters	0.66	1822	4.9	4.5
Methyl palmitate	Esters	0.66	1924	3.0	2.8
Vinyl 2-ethylhexanoate	Esters	0.86	1912	2.8	2.7
Benzyl Benzoate	Pesticides	0.93	1773	3.0	2.9
2,2,4-Trimethyl-1,3-pentanediol diisobutyrate (TXIB)	Plasticizer, Non-Phthalates	1.07	1589	2.4	2.5
2,2,4-Trimethyl-1,3-Pentanediol, 1-isobutyrate	Plasticizer, Non-Phthalates	1.03	1371	6.2	6.1
Bis(2-ethylhexyl) terephthalate (DEHT)	Plasticizer, Non-Phthalates	0.95	2744	5.7	6.3
Triacetin	Plasticizer, Non-Phthalates	1.93	1330	8.1	7.0
Tributyl phosphate	Plasticizer, Non-Phthalates	1.26	1641	2.2	2.2
Triethylene glycol di(2-ethylhexoate) (TEG-EH)	Plasticizer, Non-Phthalates	0.92	2461	7.8	7.8
Benzyl butyl phthalate (BBzP)	Plasticizer, Phthalates	1.15	2346	5.0	5.3
Bis(2-ethylhexyl) phthalate (DEHP)	Plasticizer, Phthalates	0.96	2531	5.3	5.5
Diethyl phthalate (DEP)	Plasticizer, Phthalates	1.33	1589	5.3	5.3
D7 siloxane	Siloxanes	0.52	1468	5.1	6.5
D8 siloxane	Siloxanes	0.53	1629	5.0	6.0
L10 siloxane	Siloxanes	0.50	1994	2.7	2.7
1-(1-Butoxy-2-propoxy)-2-propanol, TMS	Surfactants	0.51	1359	3.7	3.4
Diethylene glycol, 2TMS	Surfactants	0.55	1220	2.7	3.5
Diethylene glycol, n-butyl ether, trimethylsilyl ether	Surfactants	0.56	1328	4.8	4.8

[a]Compounds included are those consistently enhanced (ER > 2) across all incense samples, classified, and positively identified. [b]RI is based on linear *n*-alkanes. [c]"TMS" refers to a single trimethylsilyl group.

213 **Table S9. Total GC×GC Speciated Mass, OC, and OA Concentrations (μg m⁻³) for H3**
214 **Incense Burning Experiments.**

	Speciated mass	OC[a]	EC[b]	TC[c]	OA[d]
Lavndr-1	9.1	22.2	2.7	25.0	35.6
DougFir-1	10.8	37.2	1.1	38.3	59.5
DougFir-2	6.3	17.4	0.4	17.8	27.9
DougFir-3	9.5	31.8	1.2	32.9	50.9
DougFir-4	6.7	26.7	0.9	27.6	42.8

215 [a]OC = organic carbon; [b]EC = elemental carbon; [c]TC = total carbon
216 [d]Total organic aerosol (OA) mass is calculated using OA/OC = 1.6, as derived from Aiken et al.[10] and
217 Canagaratna et al.[11]
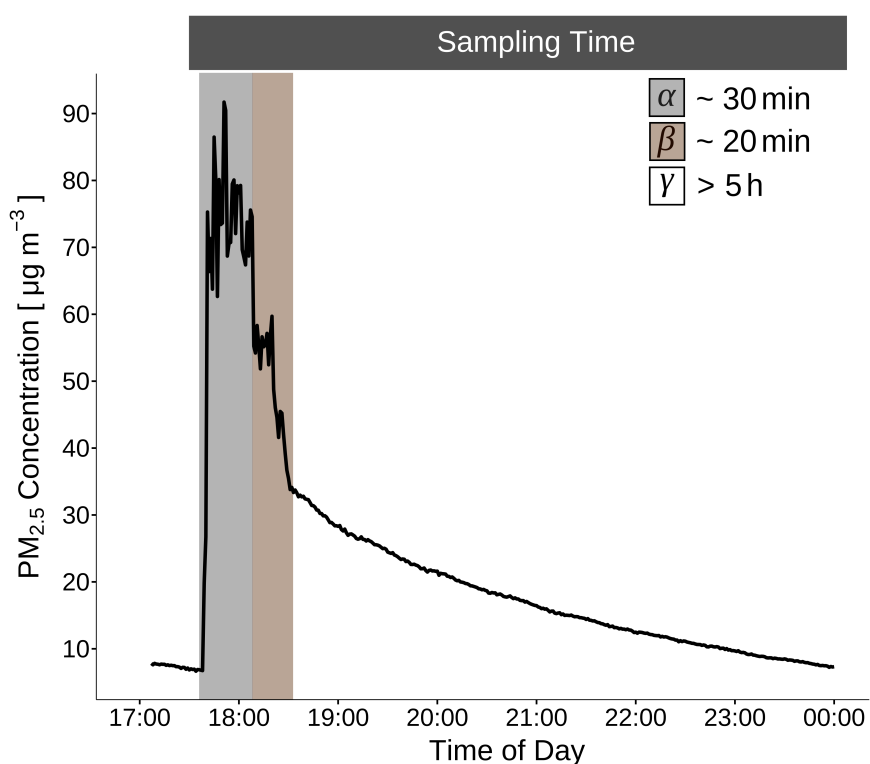
218
219 **Figure S3.** Time-resolved PM$_{2.5}$ concentrations from Particles Plus during a Douglas fir incense
220 burn, separated by three phases of mixing (α = source active, mixing incomplete; β = source
221 inactive, mixing incomplete; γ = source inactive, mixing complete).[12]

222 **Determining Incense PM$_{2.5}$ Loss (Decay) Rates**

223 The time series of PM$_{2.5}$ concentrations for the decay period, shown in Figure S3 as gamma (γ),
224 was used in calculating the total loss rate, L, by ventilation and other loss processes (e.g.,
225 deposition to indoor surfaces) during each incense burning experiment.[13] Equation (1) represents
226 a first-order mass balance, where C is incense PM$_{2.5}$ concentration, E is the PM$_{2.5}$ emission rate
227 during incense combustion, and V is the well-mixed H3 indoor volume.

228
$$\frac{dC}{dt} = -LC + \frac{E}{V} \qquad eq\ (1)$$

229 During the decay period, the incense source is inactive and so E = 0. Therefore, equation (2)
230 provides the solution to equation (1) for the gamma period, where $C(t)$ is time-resolved incense
231 PM$_{2.5}$ concentrations during the decay time, t. The total loss rate, L, is determined from the slope
232 of the regression line of the logarithm of concentration versus time shown in equation (3).

233
$$C(t) = C(0) \cdot e^{-Lt} \qquad eq\ (2)$$

234
$$\ln\big(C(t)\big) - \ln\big(C(0)\big) = -Lt \qquad eq\ (3)$$

235 **Table S10. PM$_{2.5}$ Loss Rates, L (h^{-1}), and Emission Factors, EF (mg g^{-1}), for OA in H3 Incense**
236 **Burning Experiments.**

	L (h^{-1})	EF (mg g^{-1})
Lavndr-1	0.25	7
DougFir-1	0.28	24
DougFir-2	0.27	31
DougFir-3	0.30	29
DougFir-4	0.32	23

237 **Table S11. PM$_{2.5}$ Emission Factors (mg g^{-1}) from Incense Sticks Burning Studies.**

Incense Study	EF (mg g^{-1})
Jetter et al.[14]	5.0 – 56
Lung and Hu.[15]	21 – 45
Lee and Wang.[16]	7.7 – 104
Yang et al.[17]	17 – 48
See and Balasubramanian.[18]	0.4 – 45

REFERENCES

(1) Liu, Y.; Misztal, P. K.; Xiong, J.; Tian, Y.; Arata, C.; Weber, R. J.; Nazaroff, W. W.; Goldstein, A. H. Characterizing sources and emissions of volatile organic compounds in a northern California residence using space- and time-resolved measurements. *Indoor Air* **2019**, *29*, 630–644. https://doi.org/10.1111/ina.12562.

(2) Kristensen, K.; Lunderberg, D. M.; Liu, Y.; Misztal, P. K.; Tian, Y.; Arata, C.; Nazaroff, W. W.; Goldstein, A. H. Sources and dynamics of semivolatile organic compounds in a single-family residence in northern California. *Indoor Air* **2019**, *29*, 645–655. https://doi.org/10.1111/ina.12561.

(3) Lunderberg, D. M.; Kristensen, K.; Tian, Y.; Arata, C.; Misztal, P. K.; Liu, Y.; Kreisberg, N.; Katz, E. F.; DeCarlo, P. F.; Patel, S.; Vance, M. E.; Nazaroff, W. W.; Goldstein, A. H. Surface Emissions Modulate Indoor SVOC Concentrations through Volatility-Dependent Partitioning. *Environmental Science & Technology* **2020**, *54*, 6751–6760. https://doi.org/10.1021/acs.est.0c00966.

(4) Jen, C. N.; Hatch, L. E.; Selimovic, V.; Yokelson, R. J.; Weber, R.; Fernandez, A. E.; Kreisberg, N. M.; Barsanti, K. C.; Goldstein, A. H. Speciated and total emission factors of particulate organics from burning western US wildland fuels and their dependence on combustion efficiency. *Atmospheric Chemistry and Physics* **2019**, *19*, 1013–1026. https://doi.org/10.5194/acp-19-1013-2019.

(5) Liang, Y.; Stamatis, C.; Fortner, E. C.; Wernis, R. A.; Van Rooy, P.; Majluf, F.; Yacovitch, T. I.; Daube, C.; Herndon, S. C.; Kreisberg, N. M.; Barsanti, K. C.; Goldstein, A. H. Emissions of organic compounds from western US Wildfires and their near-fire transformations. *Atmospheric Chemistry and Physics* **2022**, *22*, 9877–9893. https://doi.org/10.5194/acp-22-9877-2022.

(6) Worton, D. R.; Decker, M.; Isaacman-VanWertz, G.; Chan, A. W. H.; Wilson, K. R.; Goldstein, A. H. Improved molecular level identification of organic compounds using comprehensive two-dimensional chromatography, dual ionization energies and high resolution mass spectrometry. *Analyst* **2017**, *142*, 2395–2403. https://doi.org/10.1039/C7AN00625J.

(7) Franklin, E. B.; Yee, L. D.; Aumont, B.; Weber, R. J.; Grigas, P.; Goldstein, A. H. Ch3MS-RF: a random forest model for chemical characterization and improved quantification of unidentified atmospheric organics detected by chromatography–mass spectrometry techniques. *Atmospheric Measurement Techniques* **2022**, *15*, 3779–3803. https://doi.org/10.5194/amt-15-3779-2022.

(8) Zhang, H.; Yee, L. D.; Lee, B. H.; Curtis, M. P.; Worton, D. R.; Isaacman-VanWertz, G.; Offenberg, J. H.; Lewandowski, M.; Kleindienst, T. E.; Beaver, M. R. Monoterpenes Are the Largest Source of Summertime Organic Aerosol in the Southeastern United States. *Proceedings of the National Academy of Sciences* **2018**, *115*, 2038–2043.

276   (9)   Liang, Y.; Jen, C. N.; Weber, R. J.; Misztal, P. K.; Goldstein, A. H. Chemical composition of
277        $PM_{2.5}$ in October 2017 Northern California wildfire plumes. *Atmospheric Chemistry and*
278   *Physics* **2021**, *21*, 5719–5737. https://doi.org/10.5194/acp-21-5719-2021.

279   (10)   Aiken, A. C.; DeCarlo, P. F.; Kroll, J. H.; Worsnop, D. R.; Huffman, J. A.; Docherty, K. S.;
280   Ulbrich, I. M.; Mohr, C.; Kimmel, J. R.; Sueper, D.; Sun, Y.; Zhang, Q.; Trimborn, A.;
281   Northway, M.; Ziemann, P. J.; Canagaratna, M. R.; Onasch, T. B.; Alfarra, M. R.; Prevot, A.
282   S. H.; Dommen, J.; Duplissy, J.; Metzger, A.; Baltensperger, U.; Jimenez, J. L. O/C and
283   OM/OC Ratios of Primary, Secondary, and Ambient Organic Aerosols with High-Resolution
284   Time-of-Flight Aerosol Mass Spectrometry. *Environmental Science & Technology* **2008**, *42*,
285   4478–4485. https://doi.org/10.1021/es703009q.

286   (11)   Canagaratna, M. R.; Jimenez, J. L.; Kroll, J. H.; Chen, Q.; Kessler, S. H.; Massoli, P.;
287   Hildebrandt Ruiz, L.; Fortner, E.; Williams, L. R.; Wilson, K. R.; Surratt, J. D.; Donahue, N.
288   M.; Jayne, J. T.; Worsnop, D. R. Elemental ratio measurements of organic compounds using
289   aerosol mass spectrometry: characterization, improved calibration, and implications.
290   *Atmospheric Chemistry and Physics* **2015**, *15*, 253–272. https://doi.org/10.5194/acp-15-253-
291   2015.

292   (12)   Mage, D. T.; Ott, W. R. Accounting for Nonuniform Mixing and Human Exposure in Indoor
293   Environments. In Tichenor, B. A. (Ed.), *Characterizing Sources of Indoor Air Pollution and*
294   *Related Sink Effects, ASTM STP 1287,* American Society for Testing and Materials **1996**, No.
295   1287, pp. 263–278.

296   (13)   Chan, W. R.; Logue, J. M.; Wu, X.; Klepeis, N. E.; Fisk, W. J.; Noris, F.; Singer, B. C.
297   Quantifying fine particle emission events from time-resolved measurements: Method
298   description and application to 18 California low-income apartments. *Indoor Air* **2018**, *28*,
299   89–101. https://doi.org/10.1111/ina.12425.

300   (14)   Jetter, J. J.; Guo, Z.; McBrian, J. A.; Flynn, M. R. Characterization of emissions from burning
301   incense. *Science of The Total Environment* **2002**, *295*, 51–67. https://doi.org/10.1016/S0048-
302   9697(02)00043-8.

303   (15)   Lung, S.-C. C.; Hu, S.-C. Generation rates and emission factors of particulate matter and
304   particle-bound polycyclic aromatic hydrocarbons of incense sticks. *Chemosphere* **2003**, *50*,
305   673–679. https://doi.org/10.1016/S0045-6535(02)00613-6.

306   (16)   Lee, S.-C.; Wang, B. Characteristics of emissions of air pollutants from burning of incense in
307   a large environmental chamber. *Atmospheric Environment* **2004**, *38*, 941–951.
308   https://doi.org/10.1016/j.atmosenv.2003.11.002.

309   (17)   Yang, C.-R.; Lin, T.-C.; Chang, F.-H. Particle size distribution and PAH concentrations of
310   incense smoke in a combustion chamber. *Environmental Pollution* **2007**, *145*, 606–615.
311   https://doi.org/10.1016/j.envpol.2005.10.036.

312   (18)   See, S. W.; Balasubramanian, R. Characterization of fine particle emissions from incense
313   burning. *Building and Environment* **2011**, *46*, 1074–1080.
314   https://doi.org/10.1016/j.buildenv.2010.11.006